UK/KRCEE Doc #: P11.5 2006

Preliminary Report: Seismic Hazard Assessment At the Paducah Gaseous Diffusion Plant

Prepared by
Kentucky Research Consortium for Energy and Environment
233 Mining and Minerals Building
University of Kentucky, Lexington, KY 40506-0107

Prepared for
United States Department of Energy Portsmouth/Paducah Project Office
Acknowledgment: This material is based upon work supported by the Department of Energy under Award Number DE-FG05-03OR23032.

KRCEE

UNIVERSITY OF KENTUCKY

March 2006

UK/KRCEE Doc #: P11.5 2006

Preliminary Report: Seismic Hazard Assessment At the Paducah Gaseous Diffusion Plant

By

Zhenming Wang
Kentucky Geological Survey
228 Mining and Mineral Resources Building
University of Kentucky
Lexington, KY 40506

Edward W. Woolery
Department of Geological Sciences
309 Slone Research Building
University of Kentucky
Lexington, KY 40506

March 2006

Executive Summary

Design peak ground acceleration (PGA) of about 0.8g at the Paducah Gaseous Diffusion Plant (PGDP) is unusually high. Currently, the highest building design PGA used in California is capped at about 0.4g. These high design ground motions are not consistent with the scientific research and observations in the region. Although there are earthquakes occurring in the surrounding ereas, especially in the well-known New Madrid Seismic Zone where at least three large earthquakes (M7.0–8.0) occurred in 1811–1812, the earthquake activities are much lower in the region than those of California, Pacific Northwest, and Alaska.

There is no question that there is seismic hazard at PGDP because of its proximities to several seismic zones, particularly the New Madrid Seismic Zone. However, what level is the hazard is a difficult question. The problems in estimating seismic hazard are: 1) the difficulty in characterizing the uncertainties of seismic sources, earthquake occurrence frequencies, and ground-motion attenuations; and 2) the methods being used. "Uncertainty in seismic hazard estimates is a fact of life, even in California where seismic hazard input parameters are better known than in the CUS (central United States)." It is much more difficult to estimate seismic hazard at PGDP, because of the higher uncertainties in the input parameters.

This study shows that conservative estimates of the input parameters, i.e., the locations and maximum magnitudes of seismic zones and the ground motion attenuation relationships, were used in the national hazard maps. This study also shows that the methodology, probabilistic seismic hazard analysis (PSHA) used for the national hazard maps, contains a mathematical error in its formulations. This mathematical error has led PSHA to improperly use ground motion uncertainty (a spatial characteristic) for extrapolating return period of ground motion (a temporal characteristic). Ground motion is a consequence of earthquake and occurrence of a ground motion at a site must be associated with occurrence of an earthquake. In another words, the temporal characteristics of ground motion occurrence must be consistent with those of earthquake occurrence. This extrapolation is not appropriate and could result in an extremely high design ground motion (10g PGA or larger).

PGDP will be dominantly affected by the characteristic earthquake in the New Madrid Seismic Zone. Preliminary results from this study show that the best PGA estimate is about 0.27g, median + one standard deviation PGA of 0.54g, and median + two standard deviations PGA of 1.09g at PDGP, respectively. If occurrence of the characteristic earthquake follows Poisson distribution, the probability that this characteristic earthquake could occur in next 50 years is about 10 percent. Accordingly, the probability that the ground motion will be experienced at PGDP from the characteristic earthquake is also about 10 percent in next 50 years. The predicted ground motion at PGDP from the characteristic earthquake might be different due to the ground motion uncertainty. The best PGA estimate is 0.27g with 10 percent PE in next 50 years.

1.0 Introduction

The federal agencies, such as the Federal Emergency Management Agency (FEMA) and Environmental Protection Agency (EPA), state agencies, such as Kentucky Environmental Cabernet (KEC), and other governmental and private organizations, such as the American Association of State Highway and Transportation Officials (AASHTO) and the Building Seismic Safety Council (BSSC), use seismic hazard maps produced by the U.S. Geological Survey (Frankel and others, 1996, 2002) for seismic safety regulations and engineering designs. The maps currently being used show the ground motions with 2 percent probability of exceedance (PE) in 50 years. These maps predict very high ground motion in many counties in western Kentucky: peak ground acceleration (PGA) of 1.0 g or higher. These high ground-motion estimates have resulted in many problems in seismic safety regulations and engineering designs, and have affected everything in western Kentucky from building a single-family home to environmental clean-up at the superfund site of the Paducah Gaseous Diffusion Plant (PGDP). For example, it would not be feasible for the U.S. Department of Energy to obtain a permit from Federal and State regulators to construct a landfill at PGDP if the USGS maps with 2 percent PE in 50 years are considered. The Structural Engineers Association of Kentucky (SEAOK, 2002) also found that if the International Residential Code of 2000, which was based on the 1996 USGS maps with 2 percent PE in 50 years, is adopted in Kentucky without revision, constructing residential structures in westernmost Kentucky, including Paducah, would be impossible without enlisting a design professional.

The high ground-motion estimates by the U.S. Geological Survey (Frankel and others, 1996, 2002) are unusual, however. The 2000 International Building Code (IBC-2000), based on the 1996 USGS maps with 2 percent PE in 50 years, requires a design peak ground acceleration (PGA) of about 0.6g in Paducah, and about 0.8g at PGDP. Currently, the highest building design PGA used in California is capped at about 0.4g. These high design ground motions are not consistent with the scientific research and observations. Although there are earthquakes occurring in Kentucky and its surrounding states, especially in the well-known New Madrid Seismic Zone where at least three large earthquakes (M7.0–8.0) occurred in 1811–1812, the earthquake activities are much lower in the region than those of California, Pacific Northwest, and Alaska. Table 1 shows comparisons on the basic geological and seismological observations and design PGA between California and western Kentucky. It clearly shows that the higher design ground motion in western Kentucky does not make sense scientifically. Figure 1 show earthquakes recorded in the United States between March 23 and 29, 2006 (http://earthquake.usgs.gov/eqcenter/recenteqsus/). There are total of 553 earthquakes with magnitude 1 and greater shown in Figure 1, and only two earthquakes (magnitude between 1 and 2) occurred in the New Madrid Seismic Zone. There are 86 earthquakes with magnitude 3 and greater recorded during the period, but none of them in the New Madrid Seismic Zone. A similar patent of seismicity was observed for earthquakes with magnitude 5 or greater since 1900 (Stein and others, 2003).

Table 1. Comparisons between California and western Kentucky

	California		Western Kentucky	
Design PGA	≤0.4g (UBC97)	≤0.7g (CALTRAN)	≥0.4g (IBC-2000)	≥0.6g (bridge)
Goelogy	San Andres fault Displacement≥20 mm/y		New Madrid fault Displacement≤2 mm/y	
Seismicity	High M7-8: ~100y M6-7: ~20-50y		Low M7-8: ~500y or longer M6-7: ?	

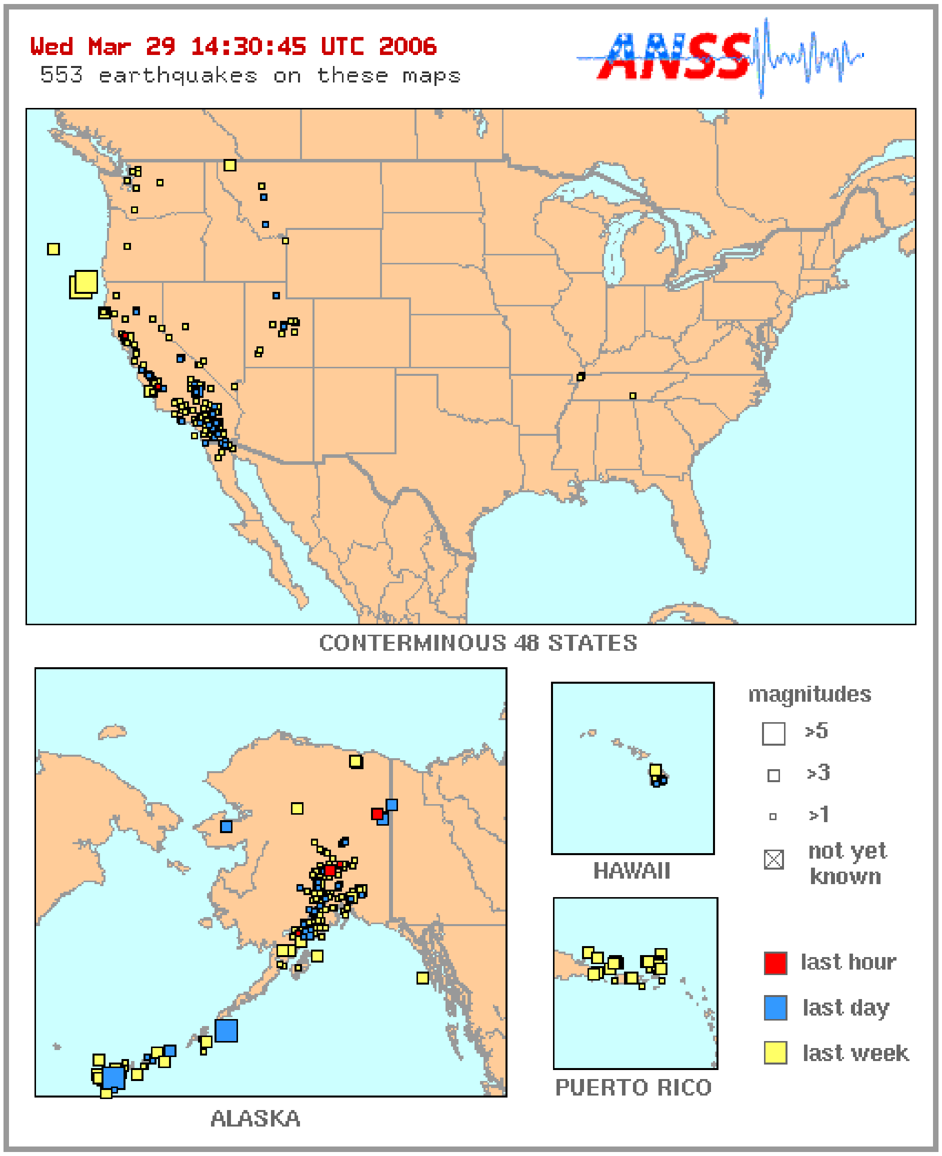

Figure 1. Seismicity in the United States between March 23 and 29, 2006.

There is no question that there are seismic hazards in western Kentucky, the Jackson Purchase region in particular, because of its proximity to the New Madrid Seismic Zone. The problems in estimating seismic hazard are 1) the difficulty in characterizing the uncertainties of seismic sources, earthquake occurrence frequencies, and ground-motion attenuation relationships and 2) the method being used. “Uncertainty in seismic hazard estimates is a fact of life, even in California where seismic hazard input parameters are better known than in the CUS (the central United States)” (Cramer, 2001). It is much more difficult to estimate seismic hazards in the central and eastern United States, including the Jackson Purchase region, because of the higher uncertainties in the input parameters.

In this report we will first review the methodologies, particularly probabilistic seismic hazard analysis (PSHA) that are commonly used for seismic hazard assessment. We will then review and determine input parameters (i.e., boundaries and maximum magnitude of the New Madrid Seismic Zone, and ground-motion attenuation relationship) for the seismic hazard assessment. Finally, we will estimate seismic hazard at PGDP.

2.0 Methodology

There are two methods, probabilistic seismic hazard analysis (PSHA) and deterministic seismic hazard analysis (DSHA), commonly used for seismic hazard assessment. PSHA and DSHA follow similar steps in estimation of seismic hazard (Reiter, 1990; Kramer, 1996):

(1) Determination of earthquake sources;
(2) Determination of earthquake occurrence frequencies – selecting controlling earthquake(s): the maximum magnitude, maximum credible, or maximum considered earthquake;
(3) Determination of ground motion attenuation relationships;
(4) Determination of seismic hazard.

The differences between PSHA and DSHA are in step (4). PSHA derives a hazard curve: a relationship between a ground motion parameter (i.e., peak ground acceleration [PGA], peak ground velocity [PGV], and response acceleration at certain periods) and its return period. DSHA determines the ground motions from a single or several earthquakes (scenarios) that have maximum impact.

Although PSHA and DSHA have been treated fundamentally different (Cramer, 2004a), as pointed out by Hanks and Cornell (1994), "in fact, PSHA and DSHA have far more in common than they do in differences, and only one fundamental difference separates the two approaches: PSHA carries units of time and DSHA doesn't. Even so, it is generally possible to associate recurrence interval information with plausible deterministic earthquakes, and when this is the case they can always be found in hazard space." Wang and others (2003, 2004) and Wang (in press a and b) showed that DSHA is a special case of PSHA. For this reason, DSHA will not be reviewed and discussed separately in this report.

2.1 PSHA

The ground motions with return periods of 500, 1,000, and 2,500 years are commonly used for general seismic safety regulation and engineering design (BSSC, 1995, 1998, 2004), and the ground motion with a return period of 10,000 years is being considered for seismic safety regulation and engineering design for nuclear facilities in the United States (NRC, 1997). The ground motions with a return period of 10,000,000 to 100,000,000 years are under consideration for seismic safety evaluation of the nuclear repository facility at Yucca Mountain, Nev. (Stepp and others, 2001; Bommer and others, 2004; Abrahamson and Bommer, 2005). What are these ground motions? Or what are these return periods? The ground motions with 10, 5, and 2 percent probability of exceedance (PE) in 50 years are other terms that are also commonly used in seismic safety regulation. What are these?

In order to better understand these, we begin with a brief review on the basic concepts and definitions of seismic hazard and risk. Seismic hazard and risk are two fundamentally different concepts (Reiter, 1990; Wang, in press a and b). Seismic hazard is a phenomenon generated by earthquakes, such as surface rupture, ground motion, ground-motion amplification, liquefaction, and induced landslides that have potential to cause harm. Seismic risk, on the other hand, is the probability (likelihood) of experiencing a level of seismic hazard or damage caused by the hazard for a given exposure (Wang and Ormsbee, 2005; Wang and others, 2005; Wang in press a and b). The exposure here means both time and societal vulnerability (i.e., building, human, etc.), but often times is incorrectly understood only either as time or societal vulnerability. For example, someone drives a car that means the driver and car (societal vulnerabilities) are exposed to a potential car crash (hazard). The probability that the driver and car could have a car crash can not be estimated without knowing how long the driver and car will be on the road. Similarly, 50 years is commonly considered as the normal life of buildings. Thus, the exposure of 50 years also implies the buildings (societal vulnerabilities) that are being exposed.

There are confusion between seismic hazard and risk (Wang and others, 2005; Wang in press a and b). The confusion causes difficulty in selecting hazard (ground-motion) level for seismic safety considerations. For example, the national seismic hazard maps, as they are being called, depict seismic hazards: i.e., ground motions and their annual frequency of exceedance (return periods (Fig. 2) (Frankel and others, 1996, 2002; Leyendecker and others, 2000). But the maps that were published are the ground motions with 10, 5, and 2 percent probability of exceedance (PE) in 50 years (Fig. 3). The 10, 5, and 2 percent PE were calculated based on the assumptions of Poisson distribution for earthquake occurrences and 50 years of building life (Frankel, 2004). Hence, the ground motions with 10, 5, and 2 percent PE in 50 years are risk maps by their definitions. These maps are called seismic hazard maps, however (Frankel and others, 1996, 2002). Only under thee assumptions of Poisson distribution for earthquake occurrences and 50 years of building life, the ground motions with 10, 5, and 2 percent PE in 50 years (risk) are equal to the ground motions with return periods of 500, 1,000 and 2,500 years (hazard), respectively.

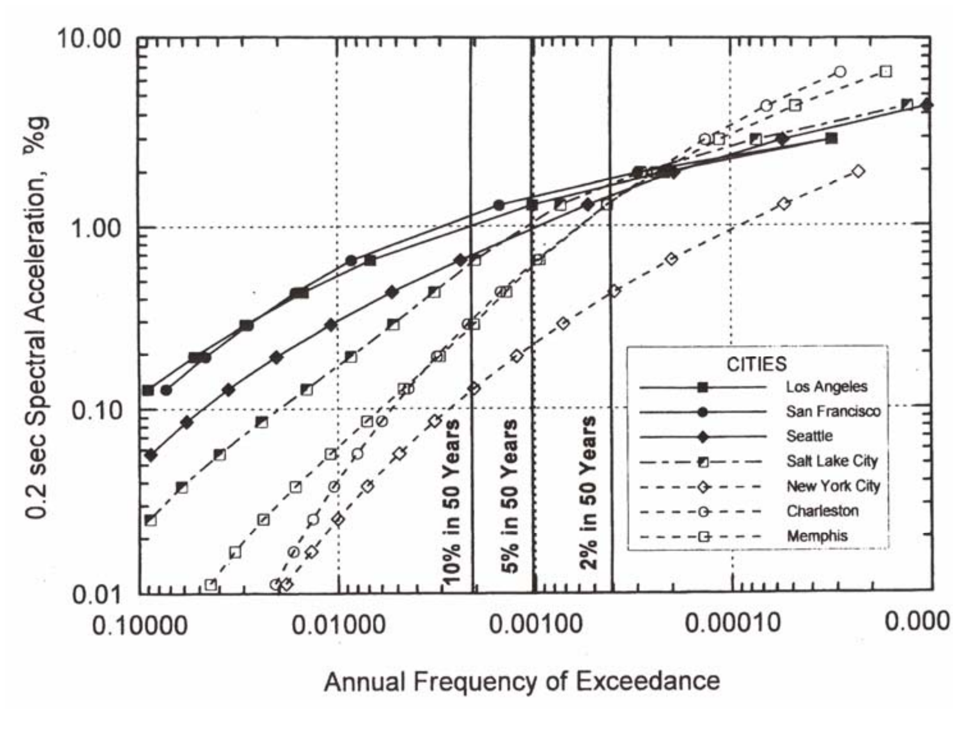

Figure 2. Harzard curves for some cities in the United States (Leyendecker and others, 2000).

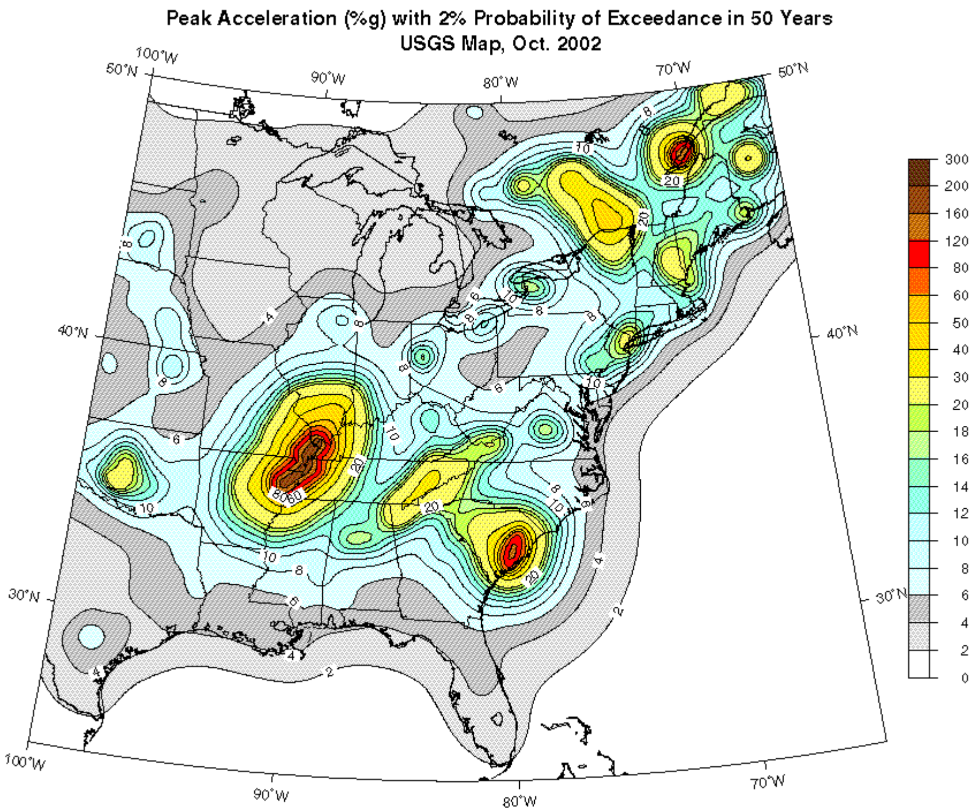

Figure 3. Peak acceleration with 2 percent PE in 50 years (Frankel and others, 2002).

2.1.1 Seismic Risk

Even though definition of seismic risk is broad and subjective, it can generally be defined as the probability of occurrence of the adverse consequences to society (Reiter, 1990). Seismic risk is quantified by three terms: the probability (likelihood), a level of seismic hazard or damage, and exposure (time and societal vulnerability). Particularly in earthquake engineering, the seismic risk was originally defined as the probability that modified Mercalli intensity (MMI) or ground motion at a site of interest will exceed a specific level at least once in a given period, a definition that is analogous to flood and wind risk (Cornell, 1968; Milne and Davenport, 1969). This definition of seismic risk in earthquake engineering is based on the assumption that earthquake occurrences follow Poisson distribution (independent of time and independent of the past history of occurrences or nonoccurrences). Although the Poisson model may not valid for describing earthquake occurrences, it is the standard model for engineering seismic risk analysis, as well as for other risk analyses such as for flood and wind.

According to Poisson model, the probability of n earthquakes of interest in an area or along a fault occurring during an interval of t years is

$$p(n,t,\tau) = \frac{e^{-t/\tau}(t/\tau)^n}{n!}, \tag{1}$$

where τ is the average recurrence interval (or average recurrence rate, $1/\tau$) of earthquakes with magnitudes equal to or greater than a specific size (M). The probability that no earthquake will occur in an area or along a fault during an interval of t years is

$$p(0,t,\tau) = e^{-t/\tau}. \tag{2}$$

The probability of one or more (at least one) earthquakes with magnitudes equal to or greater than a specific size occurring in t years is

$$p(n \geq 1,t,\tau) = 1 - p(0,t,\tau) = 1 - e^{-t/\tau} \approx 1-(1-1/\tau)^t. \tag{3}$$

Equation (3) can be used to estimate the risk, expressed as X percent PE in Y years, for a given recurrence interval (τ) of earthquakes with a certain magnitude (M) or greater. Equation (3) can also be used to calculate the average recurrence interval (τ) of earthquakes with a certain magnitude (M) or greater for a given PE in a certain years. For example, for 10, 5, and 2 percent PE in 50 years, equation (3) will result in 500-, 1,000-, and 2,500-year recurrence intervals for earthquakes, respectively.

Equation (3) determines risk in terms of earthquake magnitude (M or greater). In practice, knowing the consequences of earthquakes (i.e., ground motions or Modified Mercalli Intensity [MMI]) at a point or in a region of interest is desirable. For example, PGA and response acceleration (S.A.) at a given period are commonly needed for engineering design at a site. This is similar to the situation in flood and wind analyses whereby knowing the consequences of floods and winds, such as peak discharge and 3-s gust wind speed is desired for a specific site. The ground motions (consequences of earthquake) and their return periods: hazard curves, are determined through seismic hazard analyses (Cornell, 1968; Milne and Davenport, 1969; Frankel and others, 1996, 2002; Stein and others, 2005).

2.1.2 The Heart of PSHA

The goal of PAHS is to derive hazard curves that depict ground motions and their return periods (or annual frequencies of exceedance) (Cornell, 1968, 1971; Frankel and others, 1996, 2002). PSHA was originally developed in consideration of the uncertainty in the number, sizes, and locations of future earthquakes (Cornell, 1968). Later, Cornell (1971) extended his method to incorporate ground-motion uncertainty (i.e., the possibility that ground motion at a site could be different for different earthquakes of the same magnitude at the same distance, because of differences in source parameters and site conditions. Cornell's (1971) was coded into a FORTRAN algorithm by McGuire (1976) and became a standard PSHA.

According to Cornell (1971), McGuire (1995), and Kramer (1996), the heart of PSHA is

$$\gamma(y) = \sum_j v_j \iint P_j[Y \geq y \mid m, r] f_{M,j}(m) f_{R,j}(r) dm dr \,, \tag{4}$$

where γ is annual probability of exceedance of a ground-motion y; v_j is the activity rate; $f_{M,j}(m)$ and $f_{R,j}(r)$ are the probability density function (**PDF)** for earthquake magnitude (M) and source-to-site distance (R), respectively; and $P_j[Y \geq y \mid m, r]$ is the conditional probability that Y exceeds y (exceedance probability) for given m, r for seismic source j. Now let further examine each individual term in equation (4).

The **PDF** for source-to-site distance (R), $f_R(r)$, depends on the spatial distributions of the sources and site, and can only determined explicitly from the specific source-site geometric configuration. For example, if the source-site geometric configuration is as in Figure 4, $f_R(r)$ will be

$$f_R(r) = \frac{r}{50\sqrt{r^2 - 40^2}} \qquad 40 \leq r \leq 64 \;. \tag{5}$$

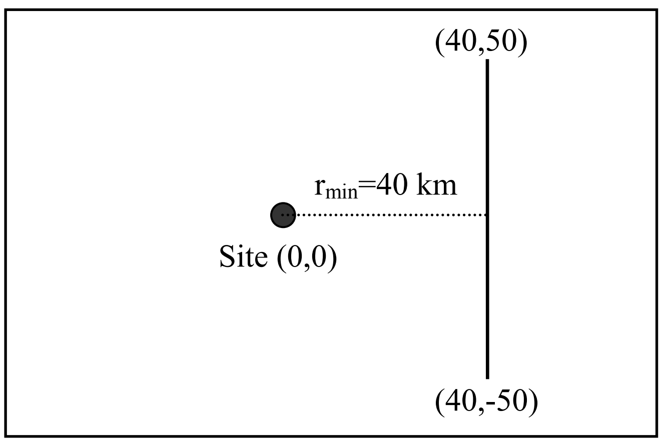

Figure 4. A hypothetical site 40 km from a line source.

The **CDF** and exceedance probability for R are

$$F_R(r) = \frac{1}{50}\sqrt{r^2 - 40^2} \qquad 40 \leq r \leq 64 \,, \tag{6}$$

and

$$P[R \geq r] = 1 - F_R(r) = 1 - \frac{1}{50}\sqrt{r^2 - 40^2} \qquad 40 \leq r \leq 64 \,, \tag{7}$$

respectively.

The **PDF** for earthquake magnitude (M) is

$$f_M(m) = \frac{\beta e^{-\beta(m-m_0)}}{1-e^{-\beta(m_{\max}-m_0)}} \qquad m_0 \le m \le m_{\max} \quad , \tag{8}$$

where β is a constant; m_0 and m_{max} are the lower and upper bounds of earthquake magnitude. Equation (8) is derived from the well-known Gutenberg-Richter distribution of

$$N = \frac{1}{\tau} = e^{\alpha-\beta m} \quad m_0 \le m \le m_{\max}\,, \tag{9}$$

where N is the cumulative number of earthquakes with magnitude equal to or greater than M occurring yearly; τ is the recurrence interval of earthquakes with magnitude equal to or greater than M; α is constant (Cornell, 1968; Kramer, 1996). In other words, $f_M(m)$ is the **PDF** for magnitude M if M follows the Gutenberg-Richter distribution (a function). Accordingly, the cumulative density function (**CDF)** for M is

$$F_M(m) = \frac{1-e^{-\beta(m-m_0)}}{1-e^{-\beta(m_{\max}-m_0)}} \qquad m_0 \le m \le m_{\max} \quad , \tag{10}$$

and the activity rate (ν) is

$$\nu = e^{\alpha-\beta m_0}\,. \tag{11}$$

The exceedance probability for M is

$$P[M \ge m] = 1 - F_M(m) = \frac{e^{-\beta[m-m_0]} - e^{-\beta(m_{\max}-m_0)}}{1-e^{-\beta(m_{\max}-m_0)}} \quad m_0 \le m \le m_{\max}\,. \tag{12}$$

In order to derive the conditional exceedance probability, $P[Y \ge y \mid m, r]$ in equation (4), we need to introduce the ground-motion attenuation relationship. In seismology, ground motion Y can be expressed as a function of magnitude (M) and source-to-site distance (R) with ground-motion uncertainty (E) (Campbell, 1981, 2003; Atkinson and Boore, 1997; Sadigh and others, 1997; Toro and others, 1997; Somerville and others, 2001)

$$\ln(Y) = f(M,R) + E\,. \tag{13}$$

The ground-motion uncertainty (E) is modeled as a log-normal distribution and quantified a standard deviation (log), $\sigma_{ln,Y}$ (Campbell,1981, 2003; Atkinson and Boore, 1997; Sadigh and others, 1997; Toro and others, 1997; Somerville and others, 2001). Figure 5 shows a general ground-motion attenuation relationship. From Figure 5, we can see that the ground motion at a given distance (r) from an earthquake of magnitude m follows a log-normal distribution and has

$$F_Y(y^*) = \int_0^{y^*} \frac{1}{\sqrt{2\pi}\sigma_{\ln,y}} \exp(-\frac{(\ln y - \ln y_m)^2}{2\sigma_{\ln,y}^2}) d(\ln(y)), \quad (14)$$

where $\sigma_{ln,y}$ is the standard deviation (log) and y_m is the median ground motion (mean in log) and equal to

$$\ln(y_m) = f(m,r). \quad (15)$$

The exceedance probability that Y^* exceeds y^*, $P[Y^* \geq y^*]$, for given m and r is

$$P[Y^* \geq y^*] = 1 - F_Y(y^*) = 1 - \int_0^{y^*} \frac{1}{\sqrt{2\pi}\sigma_{\ln,y}} \exp(-\frac{(\ln y - \ln y_m)^2}{2\sigma_{\ln,y}^2}) d(\ln(y)). \quad (16)$$

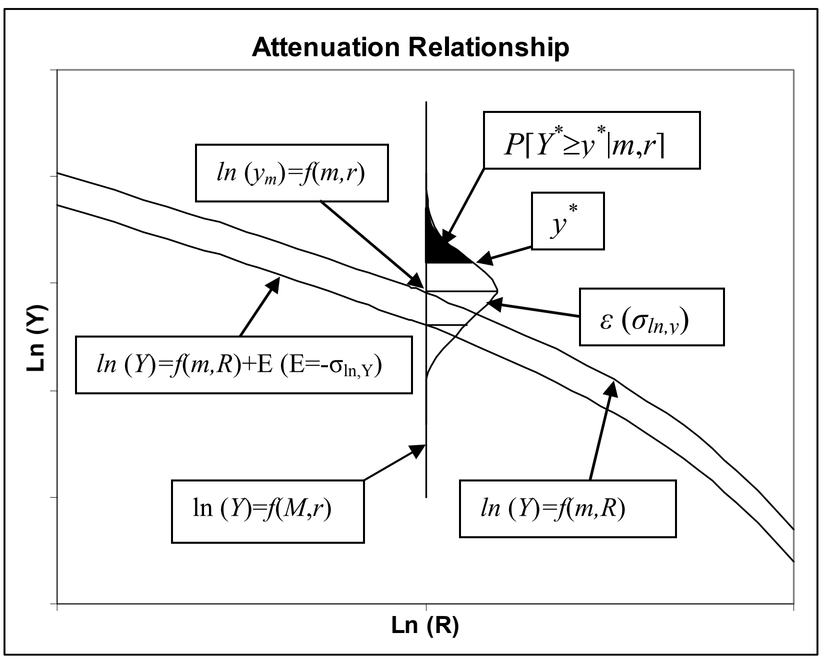

Figure 5. Ground-motion attenuation relationship for a given magnitude *m*.

In current PSHA, $P[Y \geq y \mid m, r]$ has been equated to $P[Y^* \geq y^* \mid m, r]$ (Cornell, 1971; McGuire, 1995; Kramer, 1996), i.e.

$$P[Y \geq y \mid m,r] = 1 - F_Y(y) = \int_0^{y} \frac{1}{\sqrt{2\pi}\sigma_{\ln,y}} \exp(-\frac{(\ln y - \ln y_m)^2}{2\sigma_{\ln,y}^2}) d(\ln(y)). \quad (17)$$

In other words, the conditional exceedance probability $P[Y \geq y| m, r]$ has been equated to the exceedance probability of the log-normal distribution (the ground-motion uncertainty at given m and r). As shown in equation (10), the ground motion Y is a function of earthquake magnitude (M) and source-to-site distance (R), however. The exceedance probability of the ground motion attenuation relationship should also be a function of earthquake magnitude (M) and source-to-site distance (R). This can be seen in equations (7) and (12): i.e., the exceedance probabilities for R and M are a function of R and M, respectively. The conditional exceedance probability, $P[Y \geq y |m, r]$, is equal to the exceedance probability of the ground motion attenuation relationship at given m and r, but not equal to the exceedance probability of the log-normal distribution (ground-motion uncertainty). Thus, the conditional exceedance probability, $P[Y \geq y |m, r]$, has been mistakenly equated to the exceedance probability of the ground-motion uncertainty. This mistake results in invalid formulation and causes difficulty in understanding and application of PSHA.

In current practice, the inverse of the annual probability of exceedance ($1/\gamma$), called return period (T_P), are more often used. If all seismic sources are characteristic, return period is

$$T_P(y) = \frac{1}{\sum_j \frac{1}{T_j}[1 - \int_{-\infty}^{y} \frac{1}{\sqrt{2\pi}\sigma_{\ln,c}} \exp(-\frac{(\ln y - \ln y_c)^2}{2\sigma_{\ln,c}^2})dy]}, \quad (18)$$

where T_j is the average recurrence interval of the characteristic earthquake; y_c and $\sigma_{ln,c}$ are the median ground motion and standard deviation (log) for the characteristic earthquake (m_c) at the distance (r_c) from source j. For a single characteristic source, equation (18) becomes

$$T_P(y) = \frac{T}{1 - \int_{-\infty}^{y} \frac{1}{\sqrt{2\pi}\sigma_{\ln,c}} \exp(-\frac{(\ln y - \ln y_c)^2}{2\sigma_{\ln,c}^2})dy}. \quad (19)$$

These (equations [18] and [19]) demonstrate that the mathematical error in the current PSHA, i.e., equating the exceedance probability of the ground-motion attenuation relationship (a function of m, r, and ε) to the exceedance probability of the ground motion uncertainty (ε, a log-normal distribution), results in extrapolation of the return period from the recurrence interval of earthquake and the uncertainty of ground motion (Wang and Orsmsbee, 2005; Wang, 2005a and b, in press a and b; Atkinson, in press).

Ground motion is a consequence of earthquake and occurrence of a ground motion at a site must be associated with occurrence of an earthquake. In another words, the temporal characteristics of ground motion occurrence must be consistent with that of earthquake occurrence. The current PSHA does not derive the temporal characteristics of ground motion occurrence that is consistent with that of earthquake occurrence.

2.1.3 New Approach (KY-PSHA)

Ground motions and their return periods (or annual probabilities of exceedance) can also be determined through an empirical method which derives a relationship between ground motions and their recurrence intervals from instrumental and historical records (Milne and Davenport, 1969). A similar method was recently used in seismic hazard and risk assessment in the Tokyo, Japan, area (Stein and others, 2005). As pointed out by Milne and Davenport (1969), this method may not be applicable in areas where historical data are insufficient. An alternative method was proposed by Wang (in press (a), (b)) for a single point or characteristic source.

Similar to flood occurrences (Gupta, 1989) and wind storm occurrences (Liu, 1991), earthquake occurrences follow the well-known Gutenberg-Richter magnitude-frequency relationship, equation (9). Figure 6 shows a Gutenburg-Richter curve with α=7.254 and β=2.303 for earthquakes with magnitude between M5.0 and M8.0. According to equation (9), the average recurrence intervals (τ) are 709 and 7,091 years for earthquakes of magnitude equal to or greater than 6.0 and 7.0, respectively. According equation (3), the probabilities of exceedance are 6.8 and 0.7 percent for earthquakes of magnitude 6.0 and 7.0 or greater in 50 years, respectively.

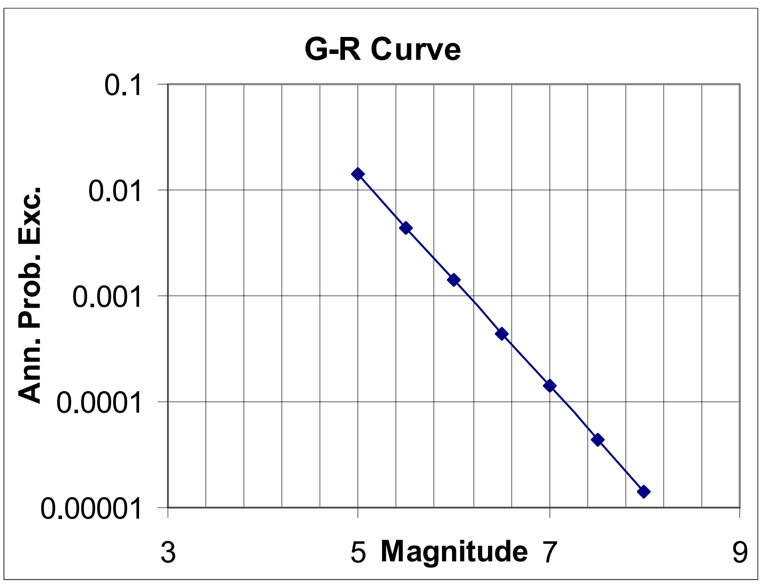

Figure 6. Gutenburg-Richter curve.

Also, from the ground-motion attenuation relationship, equations (13), we have

$$Y_E = \ln(Y) - E = f(M, R). \qquad (20)$$

Accordingly, M can be expressed in terms of R and Y_ε (ground motion with an uncertainty [$E \neq 0$]) as

$$M = M(R, Y_E), \qquad (21)$$

Normally, the ground-motion attenuation relationships are quite complicated (Campbell, 1981, 2003; Atkinson and Boore, 1997; Sadigh and others, 1997; Toro and others, 1997; Somerville and others, 2001). For example, in terms of peak ground acceleration (PGA) in the central and eastern United States, Campbell (2003) had

$$Y_E = \ln(Y) - E = 0.0305 + 0.633M - 0.0427(8.5 - M)^2 - 0.7955\ln(R^2 + [0.683\exp(0.416M)]^2) + (-0.00428 + 0.000483M)R \quad (22)$$

for $R \leq 70$ km. As shown in equation (22), the function, $M(R, Y_E)$, can not be solved analytically, but can be solved numerically. Combining equations (9) and (21) results in

$$\frac{1}{\tau} = e^{\alpha - \beta M(R, Y_E)}. \quad (23)$$

Equation (23) describes a relationship between the earthquake recurrence interval (τ) and the ground motion (Y_E) with an uncertainty (E) at distance (R). For a given $R=r$, equation (23) describes a relationship between ground motion with an uncertainty and its recurrence interval: a hazard curve. As shown in equation (9), the Gutenberg-Richter distribution generally has an upper magnitude, m_{max}, $M(R, Y_E)$ determined from equation (21) should also has the same upper magnitude. Thus, the recurrence interval determined from equation (23) also has the upper and lower limits. But the ground motions corresponding to a recurrence interval could be many because the ground-motion uncertainty. This can be seen in equation (20) in which ε can be equal to from 0, 1, 2, $3\sigma_{ln}$, or others for a given m and r.

Figure 7 shows PGA hazard curves for a site 40 km from a point source in which earthquake occurrences follow the Gutenburg-Richter relationship shown in Figure 6. In Figure 7, the median PGA's with the average recurrence intervals of 709 and 7,091 years are 0.09 and 0.2g, respectively. In terms of median PGA, equation (3) will give 6.8 and 0.7 percent PE in 50 years for 0.09 and 0.2g PGA, respectively (risk). Similarly, in terms of median$\pm\sigma$ PGA, equation (3) will give the same PE (6.8 and 0.7 percent) in 50 years for the 0.04 and 0.19g, and 0.10 and 0.39g, respectively (risk).

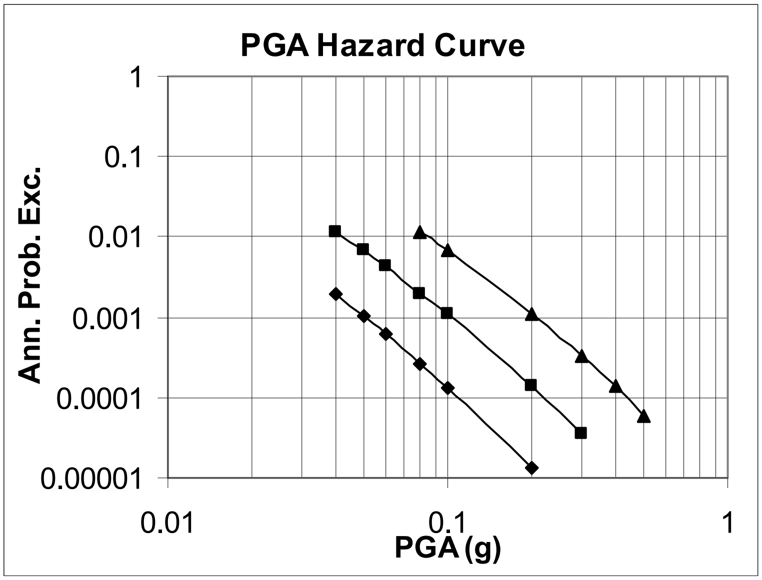

Figure 7. PGA hazard curves for a site 40 km from a point source. Square – median; Diamond – median-σ; Triangle – median+σ.

As shown above, the hazard curve in terms of ground motion can be derived directly from the Gutenburg-Richter and ground-motion attenuation relationships. This derivation [equation (23)] is only valid for a single point source or a source with constant distance, however. In general, the size and location of a future earthquake are uncertain. Uncertainties in the size and location of a future earthquake along a line source can be considered by using the *total probability theorem*. For a given $R=r$, the conditional probability that ground motion Y_E at a site exceeds y_ε is

$$P[Y_E \geq y_\varepsilon | r] = P[f(M,r) \geq y_\varepsilon] \quad . \tag{24}$$

From equations (20) and (21), we have

$$P[f(M,r) \geq y_\varepsilon] = P[M \geq M(r, y_\varepsilon)] . \tag{25}$$

From equations (12) and (25), we have

$$P[Y_E \geq y_\varepsilon \mid r] = 1 - F_M[M(r, y_\varepsilon)] = \frac{e^{-\beta[M(r,y_\varepsilon)-m_0]} - e^{-\beta(m_{\max}-m_0)}}{1 - e^{-\beta(m_{\max}-m_0)}} \quad . \tag{26}$$

According to the *total probability theorem*, the probability that ground motion Y_E at the site exceeds a given y_ε from a line source is equal to

$$P[Y_E \geq y_\varepsilon] = \int P[Y_E \geq y_e \mid r] f_R(r) dr = \int \frac{e^{-\beta[M(r,y_\varepsilon)-m_0]} - e^{-\beta(m_{\max}-m_0)}}{1 - e^{-\beta(m_{\max}-m_0)}} f_R(r) dr . \tag{27}$$

The average annual probability that ground motion Y_E at the site exceeds a given y_ε from a line source is equal to

$$\nu P[Y_E \geq y_\varepsilon] = \nu \int \frac{e^{-\beta[g(r,y_\varepsilon)-m_0]} - e^{-\beta(m_{\max}-m_0)}}{1-e^{-\beta(m_{\max}-m_0)}} f_R(r)dr \,. \tag{28}$$

For all sources, the total average annual probability that ground motion Y_E at the site exceeds a given y_ε is equal to

$$\gamma(y_\varepsilon) = \sum_j \nu_j P_j[Y_E \geq y_\varepsilon] = \sum_j \nu_j \int \frac{e^{-\beta_j[g_j(r,y_\varepsilon)-m_0]} - e^{-\beta_j(m_{\max}-m_0)}}{1-e^{-\beta_j(m_{\max}-m_0)}} f_{R,j}(r)dr \,. \tag{29}$$

If all sources are characteristic, equation (29) will become

$$\gamma(y_\varepsilon) = \sum_j \nu_j P_j[Y_E \geq y_\varepsilon] = \sum_j \nu_j \frac{e^{-\beta_j[M_{C,j}-m_0]} - e^{-\beta_j(m_{\max}-m_0)}}{1-e^{-\beta_j(m_{\max}-m_0)}} \,. \tag{30}$$

For a single characteristic source, equation (30) becomes

$$\gamma(y_\varepsilon) = e^{\alpha-\beta M_C} = \frac{1}{T} \,. \tag{31}$$

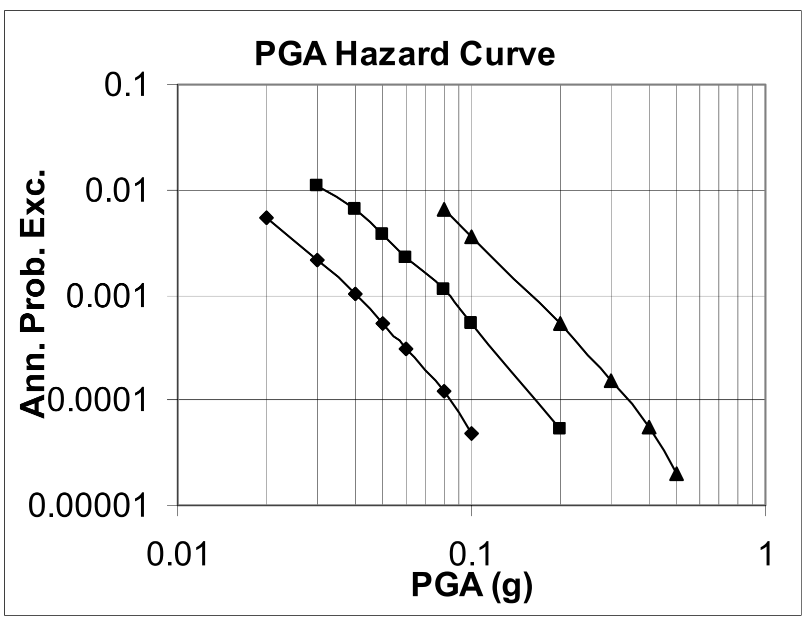

Figure 8. PGA hazard curves for a site 40 km from a line source. Square – median; Diamond – median-σ; Triangle – median+σ.

As shown in Figure 6, the recurrence intervals of earthquakes vary from about 100 years for earthquakes equal to or greater than 5.0, to 10,000 years for earthquakes equal to or greater than 8.0. These intervals determine that the range of return periods of the ground motions should also be between 100 and 10,000 years, because the ground motions are the consequences of those earthquakes. The new approach derives the ground motions with the return periods of between 100 and 10,000 years (Figs. 7, 8). Therefore, in terms of temporal characteristics, the outputs from the new approach are consistent with the inputs. Particularly in the case of a single characteristic source, the output return period is equal to the input recurrence interval.

In order to differentiate this new approach from current PSHA, we call this new approach as KY-PSHA. KY-PSHA can be easily expanded to consider the non-unique interpretations of seismological parameters, which are commonly characterized by a logic-tree in PSHA (SSHAC, 1997; Stepp and others, 2001; Scherbaum and others, 2005).

3.0 Seismic Sources

The causes of the intraplate earthquakes in the central United States are not well understood (Braile and others, 1986; Zoback, 1992; Newman and others, 1999; Kenner and Segall, 2000). Two hypotheses have been proposed to explain this seismicity: (a) selective reactivation of preexisting faults by local variations in pore pressure, fault friction and/or strain localization along favorably orientated lower crustal ductile shear zones formed during earlier deformation (Zoback *et al*., 1985); and (b) local stress perturbations which may produce events incompatible with the regional stress field (Zoback *et al*., 1987). In the central and eastern United States the regional stress field is reasonably well known from well-constrained focal mechanisms (e.g., Herrmann and Ammon, 1997), yet, the link between the stress field and the contemporary seismicity remains enigmatic. In fact, many dramatically different seismic source zones have been proposed and used in the seismic hazard estimates in the central United States (EPRI, 1988; Bernreuter and others, 1989; REI, 1999; Geomatrix Consultants, Inc., 2004). Seismic source zones considered in this study are discussed bellow.

3.1 New Madrid Seismic Zone

The New Madrid Seismic Zone is a tightly clustered pattern of earthquake epicenters that extends from northeastern Arkansas into northwestern Tennessee and southeastern Missouri (Figure 4). Earthquakes along the northeast trending alignment of earthquakes in northeastern Arkansas and those events in southeastern Missouri between New Madrid and Charleston, Missouri, are predominately right-lateral strike-slip events. Whereas the earthquakes along the northwesterly trend of seismicity extending from near Dyersburg, Tennessee, to New Madrid, Missouri, are predominately dip-slip events. Focal depths of the earthquakes in the New Madrid Seismic Zone typically range between 5 and 15 km (Chiu *et al*., 1992). Even though it has been well studied, the locations and maximum magnitude of New Madrid Faults are still uncertain. These can be seen in the USGS national hazard maps (Frankel and others, 1996 and 2002).

"To calculate the hazard from large events in the New Madrid area we considered three parallel faults in an S-shaped pattern encompassing the area of highest historic seismicity (Fig. 10). These are not meant to be actual faults; they are simply a way of expressing the uncertainty in the source locations of large earthquakes such as the 1811-12 sequence. The extent of these fictitious faults is similar to those used in Toro and others (1992). We assumed a characteristic rupture model with a characteristic moment magnitude **M** of 8.0, similar to the estimated magnitudes of the largest events in 1811-12 (Johnston, 1996a, b). A recurrence time of 1000 years for such an event was used as an average value, considering the uncertainty in the magnitudes of prehistoric events"- (Frankel and others, 1996). These were the New Madrid faults used in the 1996 USGS national hazard maps. However, in the 2002 USGS national hazard maps, quite different parameters for the New Madrid faults were used (Frankel and others, 2002): "The 2002 update incorporates a shorter mean recurrence time for characteristic earthquakes in New Madrid than was used in the 1996 maps, as well as a smaller median magnitude than that applied in 1996. A logic tree was developed for the characteristic magnitude (Mchar) and the configuration of the sources of the characteristic earthquakes, where the uncertainty in location is described by using three fictitious fault sources as in the 1996 maps. A mean recurrence time of 500 years for characteristic earthquakes is used in the calculations

(Cramer, 2001). This was based on the paleoliquefaction evidence of two to three previous sequences prior to the 1811-12 events (Tuttle and Schweig, 2000)."

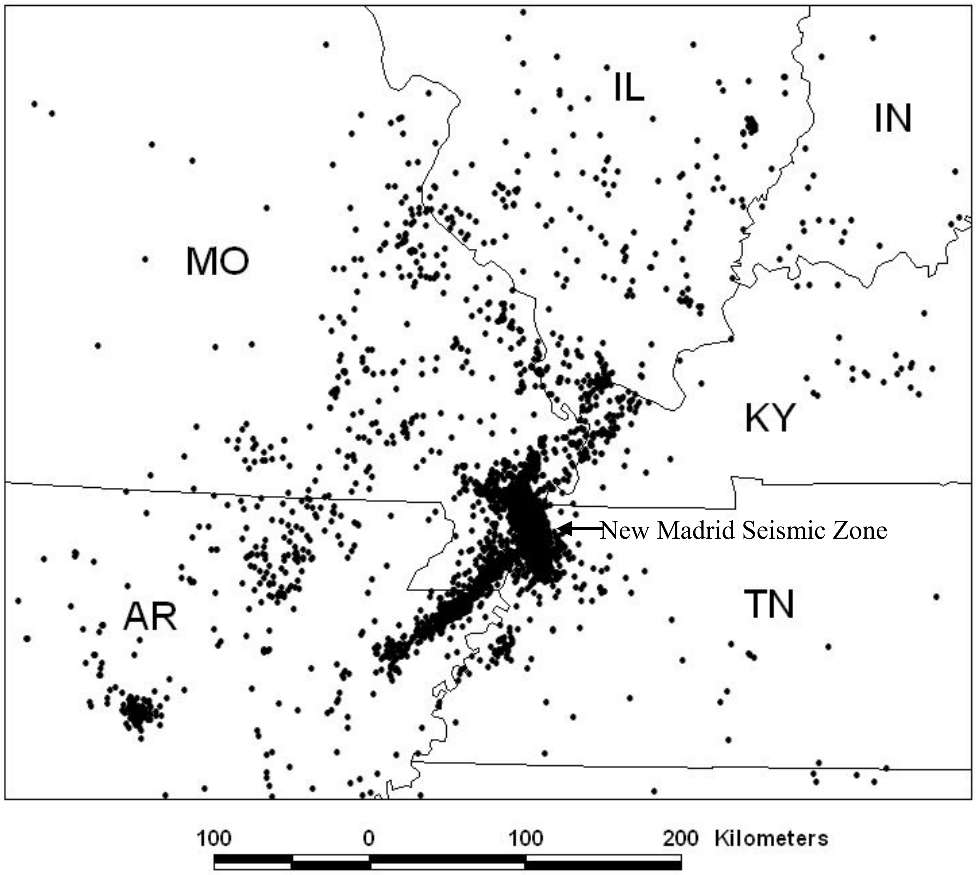

Figure 9. Seismicity between 1974 and 2005 in the central United States (CERI, 2005).

As shown in Figure 10, the northern extension of the New Madrid faults has significant effect on seismic hazard estimates at PGDP. Although many researchers postulated that the New Madrid faults probably extend northeast into the Jackson Purchase region in western Kentucky, even into southern Illinois (Wheeler, 1997; REI, 1999), there are consistent geologic and seismologic evident indicating that a northwest trending structure separating the southern Illinois seismic zone from the New Madrid zone (Braile and others, 1997; Wheeler, 1997). This can be seen clearly in Figure 11 which shows the Bouguer gravity anomaly and 1974-94 earthquake epicenters in the New Madrid region (Braile and others, 1997).

As suggested by Wheeler (1997), the northeast extensions of the New Madrid faults can be substantiated by further seismic network monitoring. Recent studies (Wang and others, 2003b; Horton and others, 2005; Anderson and others, 2005) indicated that the New Madrid faults may not extend northeast into the Jackson Purchase region. A dense seismic network of nine stations was installed in the Jackson Purchase region (Fig. 12) in late 2002 (Wang and others, 2003b). Table 2 lists the earthquakes recorded by the dense seismic network between January 2003 and June 2005 (Anderson and others, 2005). The focal depths of these earthquakes are all less then

10 km. It is interesting that the June 6, 2003, Bardwell, Kentucky, event (M_W4.0) is extremely shallow, only about 2 km, with southeast-northwest maximum compression (Horton and others, 2005). These short period and dense network observations suggests the characteristics of earthquakes in the Jackson Purchase region, are different from those of earthquakes in the central New Madrid Seismic zone. In other words, the short period seismic observations suggest the New Madrid faults may not extend into the Jackson Purchase region. A recent study by Baldwin and others (2005) showed that the New Madrid North faults are coincident with current seismicity in southeastern Missouri.

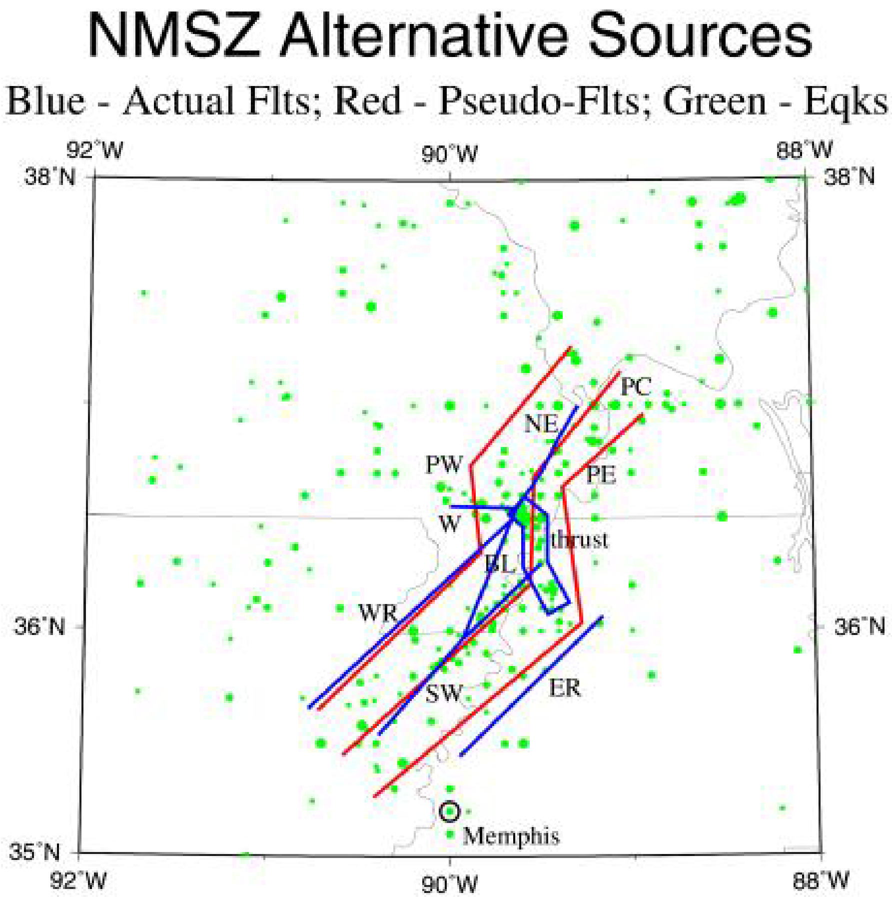

Figure 10. New Madrid Faults (Cramer, 2004b). Pseudo-faults (red) were used in the 1996 and 2002 USGS seismic hazard maps (Frankel and others, 1996, 2002).

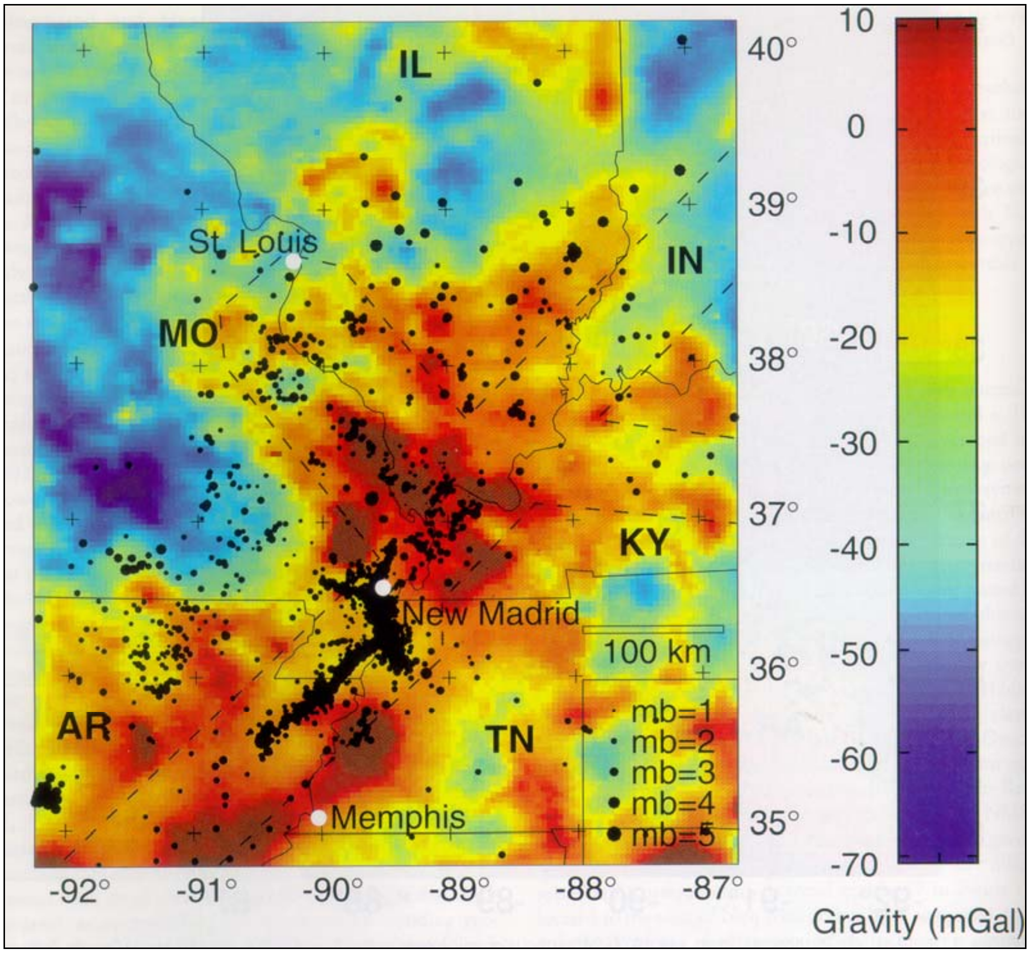

Figure 11. Bouguer gravity anomaly and 1974-94 earthquake epicenters and the New Madrid rift complex (Braile and others, 1997).

Table. 2. Parameters of earthquakes.

Date	Time	Lat.	Long.	Depth	Magnitude	Depth (UK)
06/06/03	12:29:34	36.870	-88.980	2.6	4	1.5
08/26/03	2:26:58	37.100	-88.680	1.9	3.1	2.0
02/12/04	6:49:49	37.110	-88.960	27.2	2.4	9.8
06/20/05	2:00:32	36.930	-88.990	9.8	2.7	8.7
06/20/05	12:21:42	36.920	-89.000	21.0	3.6	8.9

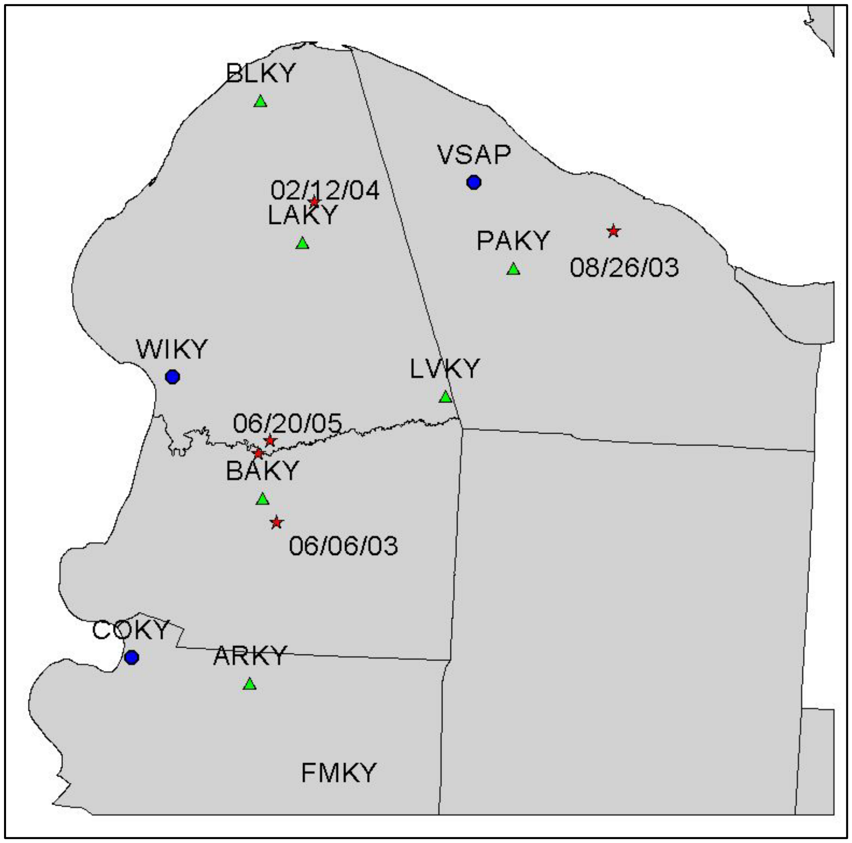

Figure 12. Dense seismic network and earthquakes recorded between January 2003 and June 2005 in the Jackson Purchase region.

The other large uncertainty for the New Madrid Seismic Zone is estimate of the maximum magnitude. A single moment magnitude of **M**8.0 was used in the 1996 national maps (Frankel and others, 1996), while a Mchar logic tree was used in the 2002 national maps for New Madrid Seismic Zone: **M**7.3 (0.15 wt), **M**7.5 (0.2 wt), **M**7.7 (0.5 wt), **M**8.0 (0.15 wt) (Frankel and others, 2002). More recent studies (Hough and others, 2000; Bakun and Hopper, 2002; Pujol and Pezeshk, 2005) suggested that the magnitude is about **M**7.2-7.5. GPS observations also suggested a similar magnitude (**M**7.2-7.5) (Newman and others, 2000; Calais and others, 2005).

Although there are large uncertainties in the locations of the New Madrid fault and the associated maximum magnitude, there is a general agreement among the scientists that the location of the New Madrid fault outlined by Johnston and Scwheig (1996) is more realistic (Cramer, 2004b). The recent studies also suggested that the maximum magnitude for the New Madrid Seismic Zone is in the range of **M**7.2-8.0. In this report, we will use the location of the New Madrid fault given by Johnston and Schweig (1996) with a maximum magnitude of **M**7.7.

3.2 Wabash Valley - Southern Illinois Seismic Zone

Nuttli and Herrmann (1978) first proposed the seismic zone on the basis of (1) the number of earthquakes, (2) the occurrence of five ≥5 $m_{b,Lg}$ earthquakes in the seismic zone between 1875 and 1975, and (3) the presence of the Wabash Valley Fault Zone. The boundaries of the Wabash Valley Seismic Zone as drawn by Wheeler and Frankel (2000) are shown in Figure 13. Also included in the figure are the epicentral locations of the damaging (MMI≥VI) earthquakes in the seismic zone (Stover and Coffman, 1993), and the location of the 5.1 $m_{b,Lg}$ September 27, 1909, earthquake that occurred just north of the seismic zone. Dates, times, and epicentral locations of the damaging earthquakes shown in Figure 13 are listed in Table 3. Unlike the seismicity in the New Madrid Seismic Zone, where there is a well defined pattern of seismicity, seismicity in the Wabash Valley Seismic Zone is diffused over a broad area.

Despite the number of damaging earthquakes in the Wabash Valley Seismic Zone, there has never been an adequate number of permanent seismograph stations in the seismic zone to, in general, derive well-constrained focal depths or focal mechanisms. As previously indicated, of the 18 events listed in Table 3, the only events for which well determined focal depths and focal mechanisms have been estimated, are events 15, through 18. These four earthquakes were large enough to generate sufficient surface waves data that their focal depths and focal mechanisms could be estimated using the radiation pattern of their Rayleigh and Love waves (Herrmann and Ammon, 1997).

TABLE 3. DAMAGING EARTHQUAKES IN THE WABASH VALLEY SEISMIC ZONE

Event No.	Date (Mo-Day-Yr)	Time (GMT)	Lat./Long. (°N/°W)	$m_{b,Lg}$[1]	Magnitude M_w[2]	(km)	Depth[3]
1.	July 5, 1827		38.0/87.5	4.8	4.4		
2.	Aug. 7, 1827	4:30	38.0/88.0	4.8	4.4		
3.	Aug. 7, 1827	7:00	38.0/88.0	4.7	4.3		
4.	Sep. 25, 1876	6:00	38.5/87.8	4.5	4.1		
5.	Sep. 25, 1876	6:15	38.5/87.8	4.8	4.4		
6.	Feb. 6, 1887	22:15	38.7/87.5	4.6	4.2		
7.	July 27, 1891	2:28	37.9/87.5	4.1	3.7		
8.	Sep. 27, 1891	4:55	38.25/88.5	5.5	5.3		
9.	Apr. 30, 1899	2:05	38.5/87.4	4.9	4.6		
10.	Sep. 27, 1909	9:45	39.8/87.2	5.1	4.8		
11.	Nov. 27, 1922	3:31	37.8/88.5	4.8	4.4		
12.	Apr. 27, 1925	4:05	38.2/87.8	4.8	4.4		
13.	Sep. 2, 1925	11:56	37.8/87.5	4.6	4.2		
14.	Nov. 8, 1958	2:41	38.44/88.01		4.4	4.0	
15.	Nov. 9, 1968	17:01	37.91/88.37		5.5	5.3	22
16.	Apr. 3, 1974	23:05	38.55/88.07		4.5	4.3	14
17.	June 10, 1987	23:48	38.71/87.95		5.1	5.0	10
18.	June 18, 2002	18:37	37.98/87.78		4.9	4.5	17-19

1. **Magnitudes ($m_{b,Lg}$) are from Stover and Coffman (1993) except for events 8 and 15. Street (1980) gave a magnitude range of 5.5 to 5.8 $m_{b,Lg}$ for the September 27, 1891, event, based on an analysis of all the MM intensity data, whereas Stover and Coffman's (1993) $m_{b,Lg}$ of 5.2 is based solely upon the felt area. The 5.5 $m_{b,Lg}$ for event 17, the November 9, 1968, southern Illinois event, is more generally accepted than the 5.3 $m_{b,Lg}$ given by Stover and Coffman (1993). The $m_{b,Lg}$ magnitude, seismic moment, and epicentral location for event 18 are preliminary estimates based on data from the University of Kentucky Seismic and Strong-Motion Network and R. Herrmann at Saint Louis University (personal communication).**

2. **Except for events 15, 16, and 17, moment magnitudes (M_w) were derived using the m_b to seismic moment (M_o) to moment magnitude conversion outlined in Appendix A. Moment magnitudes of events 17, 18, and 19 were calculated using the seismic moments given in Herrmann and Ammon (1997).**

3. **Focal depths are from Herrmann and Ammon (1997), except event 18, which is based on a personnel communication from R.B. Herrmann.**

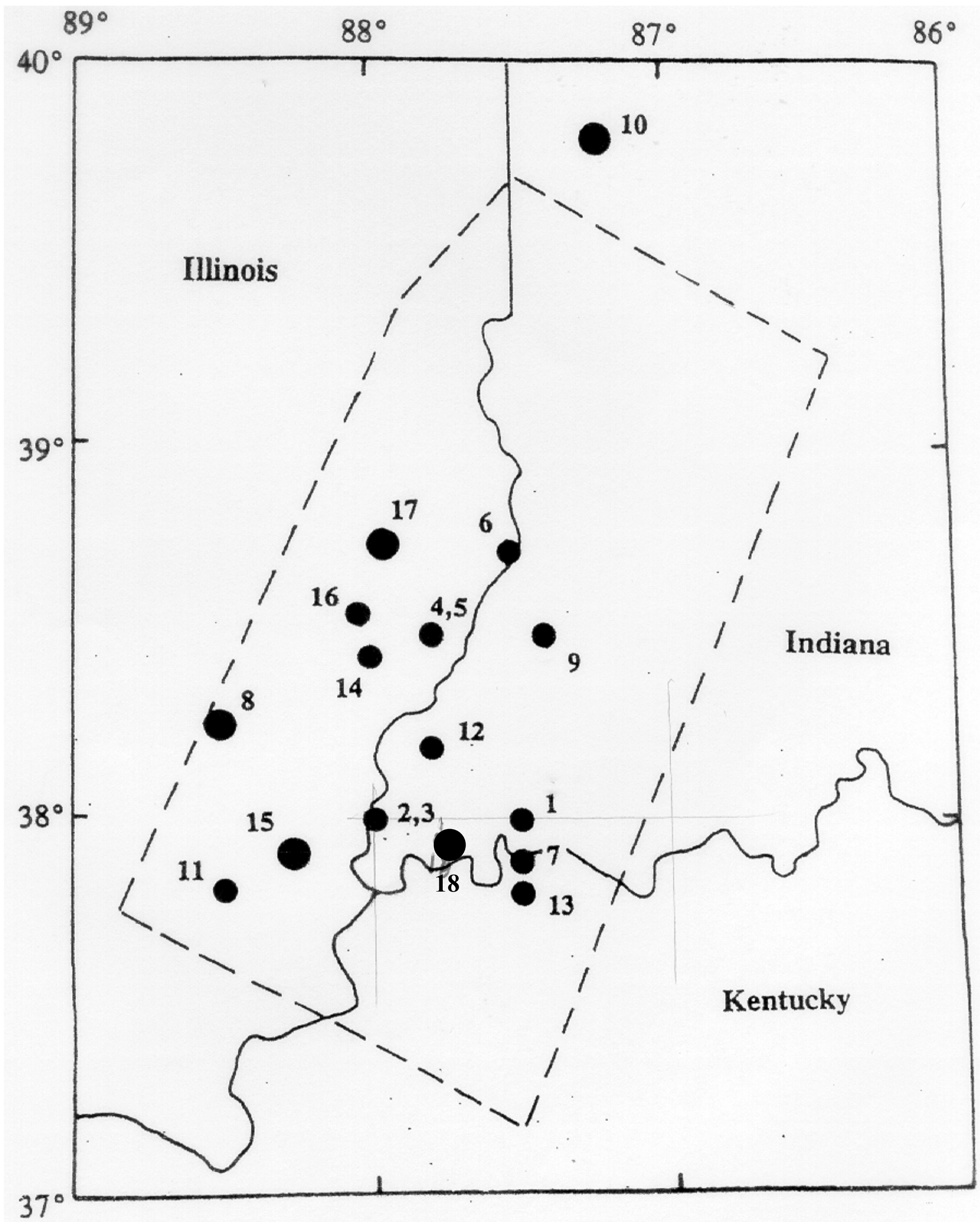

Figure 13. Epicentral locations of the damaginf earthquakes in the Wabash Valley Seismic Zone.

The largest instrumentally recorded historical earthquake in the Wabash Valley Seismic Zone is the November 9, 1968, earthquake (event 15 in Table 3). McBride *et al*. (2002) believes that the November 9, 1968, earthquake occurred as a result of the reactivation of a fault plane within a series of moderately dipping lower crustal reflectors that are decoupled from the overlying Paleozoic structure. The June 18, 2002, Dartmat, Ind., earthuquake (M4.6) was well located (Table 3). Kim (2003) also believes that the June 18, 2002, earthquake occurred as a result of the reactivation of a fault within the Wabash Valley fault system (Fig. 14)

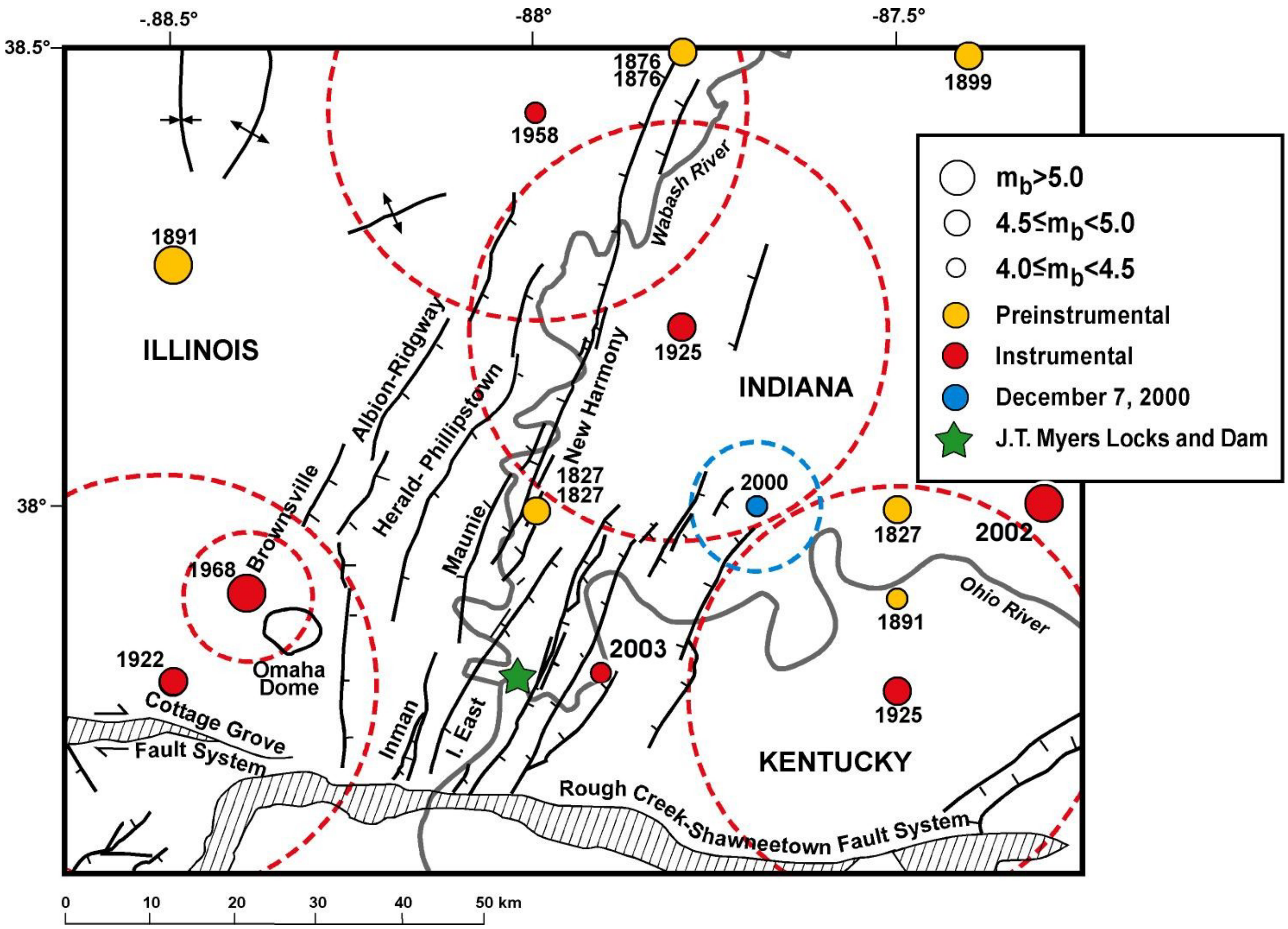

Figure 14. Earthquakes and faults in the lower Wabash Valley.

The Wabash Valley fault system shown in Figure 14, is a series of north-norteast trending normal faults with right-lateral offsets across the Herald-Pillipstown and the New Harmony faults. The locations and extent of faulting are well known from the extensive set of drill logs and seismic reflection lines acquired for oil and gas exploration purposes. Between the Albion-Ridgway and New Harmony faults is the Grayville Graben, so named by Sexton *et al*. (1996) and shown by Bear *et al*. (1997) as exhibiting Cambrian extensional slip. Based on Bear *et al.'s* (1997) interpretation of the fault movement, Wheeler and Cramer (2002) identify the Grayville Graben as Iapetan. However, they all but dismiss the graben and the Wabash Valley fault system as being seismogenic.

As discussed above, there is no clear evident to directly link anyone of the earthquakes to the faults in the Wabash Valley Seismic Zone. Thus, the Wabash Valley Seismic Zone was treated as an aerial source in the seismic hazard analyses (Frankel and others, 1996, 2002; Wheeler and Frankel, 2000). The maximum magnitude of M7.5 was assigned to the zone in the national seismic hazard maps (Frankel and others, 1996, 2002; Wheeler and Frankel, 2000), which was based on the magnitude estimates from paleo-liquefaction studies by Obermeier and others (1991, 1992), Munson and others (1992, 1997), and Pond and Martin (1997). However, recent studies by Street and others (2004) and Olson and others (2005) suggested that the best estimates of those paleo-earthquakes are in the range of 6.2-7.3. In this study, the tristate seismic source zone, one of the alternative source zones suggested by Wheeler and Cramer (2002) for the Wabash Valley Seismic Zone, will be used in this study. We assign a maximum magnitude of M6.8 to the Wabash Valley Seismic Zone.

3.3 Background Seismicity

Earthquakes occurred throughout Kentucky and its surrounding states, many of them are not associated with any known seismic zone or geologic/tectonic feature. For example, the February 28, 1854, earthquake ($m_{b,Lg}$4.0) occurred in the Central Kentucky that is not associated with any known seismic zone. Many of those earthquakes were recorded by the University of Kentucky seismic network since 1984 (Street and Wang, 2003). These earthquakes are defined as background seismicity. In this study, an event of $m_{b,Lg}$4.5 is assumed to be the background earthquake that could occur anywhere in Kentucky with exception of the 28 highlighted counties (Fig. 15). This background earthquake was used in the KTC-96-4 report and maps (Street et al., 1996).

The maximum magnitude of the background earthquake in the eight counties in western Kentucky (Ballard, Carlisle, Fulton, Graves, Hickman, Livingston, Marshall, and McCracken) is 5.3 $m_{b,Lg}$. This magnitude is based on the counties' proximity to the New Madrid Seismic Zone, moderate size historical events, and occasional events within the counties which have been recorded by the University of Kentucky Seismic Network, such as the June 6, 2003, Bardwell, Ky., earthquake (Wang et al., 2003b). Within the eight counties, there were many earthquakes measuring 3.0 $m_{b,Lg}$ or larger have been recorded, such as the June 6, 2003, Bardwell, Ky., earthquake (M4.0). The Bardwell earthquake caused some damages in Bardwell.

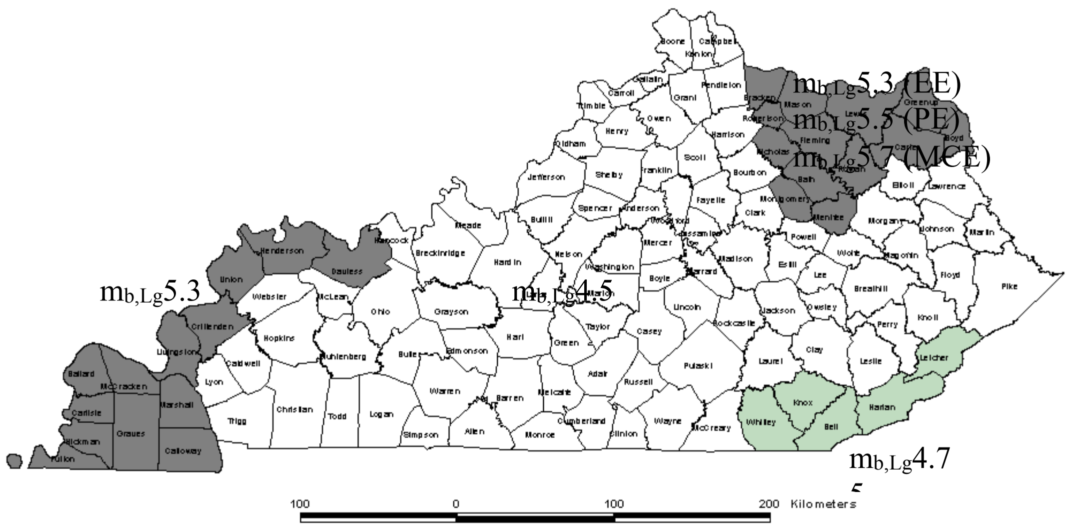

Figure 15. Background earthquakes in Kentucky

4.0 MAGNITUDE-RECURRENCE RELATIONSHIP

In the central United States, the seismicity is relative low, in comparison with California. There is no instrumental recordings on strong and large earthquakes (M>6.0). There are only two strong historical events (6.0<M<6.5), the 1843 Marked Tree, Ark., earthquake (M6.0) and the 1895 Charleston, Missouri., earthquake (M6.0) (Bakun et al., 2003), and the 1811-12 New Madrid great events (7.0<M<8.0). Bakun et al. (2003) also suggested that the 1895 Charleston, Missouri, earthquake was located in southern Illinois, about 100 km north of Charlston (not in the New Madrid Seismic Zone). The instrumental and historical records are insufficient to construct the magnitude-occurrence relationships in the central United States. Prehistoric records (paleo-liquefactions) has been used in constructing the magnitude-occurrence relationships. Figure 16 and 17 show the magnitude-occurrence relationships for the New Madrid Seismic Zone (Frankel *et al*., 1996) and the Wabash Valley Seismic Zone (Wheeler and Cramer, 2002) based on the instrumental, historical, and paleo-liquefaction records.

Figure 16 shows that 1) the annual rate derived from instrumantal and historical earthquakes is not consistent with that derived from paleo-liquefaction records; 2) there is a lack of strong earthquakes of M6.0-7.0 or an earthquake deficit in the New Madrid Seismic Zone. A *b*-value of 0.95 was used in the USGS national seismic hazard mapping for the central United States (Frankel et al., 1996, 2002). Based on the instrumantal and historical records, the annual occurrence of a M7.5 earthquake is less than 0.0001 (reccurence interval is longer than 10,000 years) in the New Madrid Seismic Zone (Fig. 16). However, the paleoliquefaction records revealed an annual occurrence of 0.00218 (reccurence interval of about 459 years) for a M7.7 earthquake in the New Madrid Seismic Zone (Fig. 16). These large earthquakes were commonly treated as characteristic events (Frankel et al., 1996, 2002; Geomatrix Consultants, Inc., 2004). In this study, we assign a magnitude of M7.7 with a mean recurrence interval of 500 years for the characteristic event along the New Madrid fault.

The paleo-liquefaction studies by Obermeier and others (1991, 1992), Munson and others (1992, 1997), and Pond and Martin (1997) suggested a mean recurrence interval of about 6,000 years for the large prehistoric earthquakes in the Wabash Valley Seismic Zone. As shown in Figure 17, this recurrence interval is consistent with those projected from the seismicity of small and moderate earthquakes (≤M5.0) (Wheeler and Cramer, 2002). From Figure 17, we can get a recurrence interval of about 2,500 years for earthquake with magnitude 6.8 or greater. This recurrence interval will be used for the Wabash Valley Seismic Zone in this report.

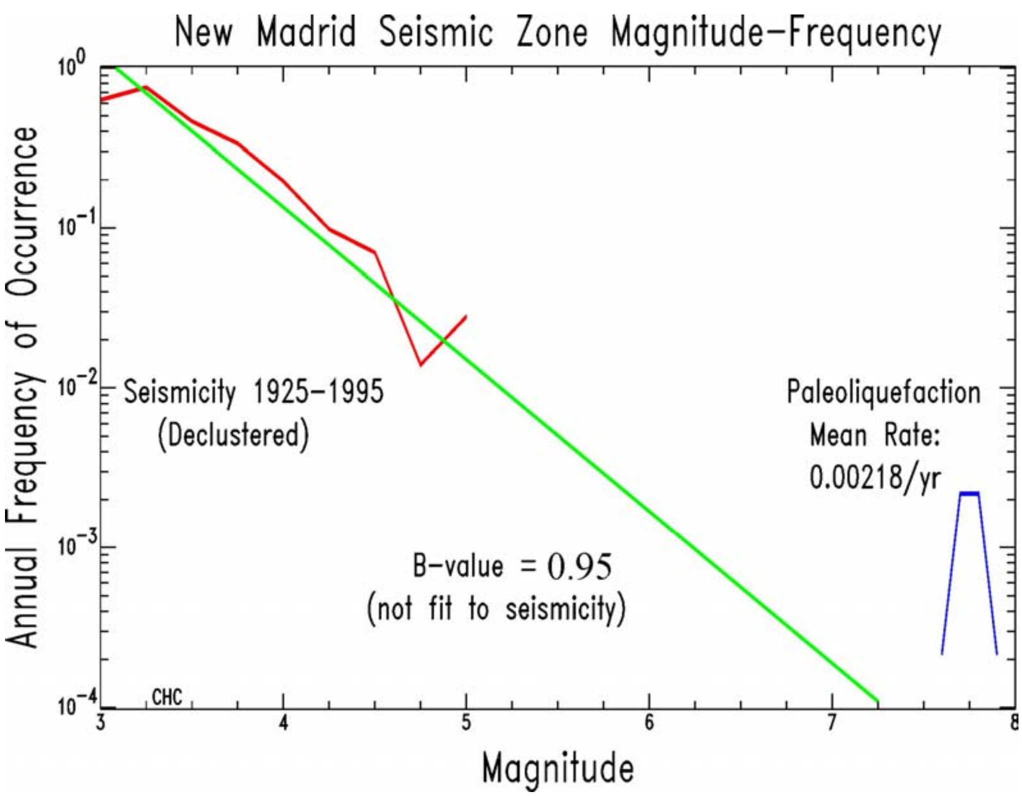

Figure 16. Magnitude-frequency relationship in the New Madrid Seismic Zone (Frankel, 1996).

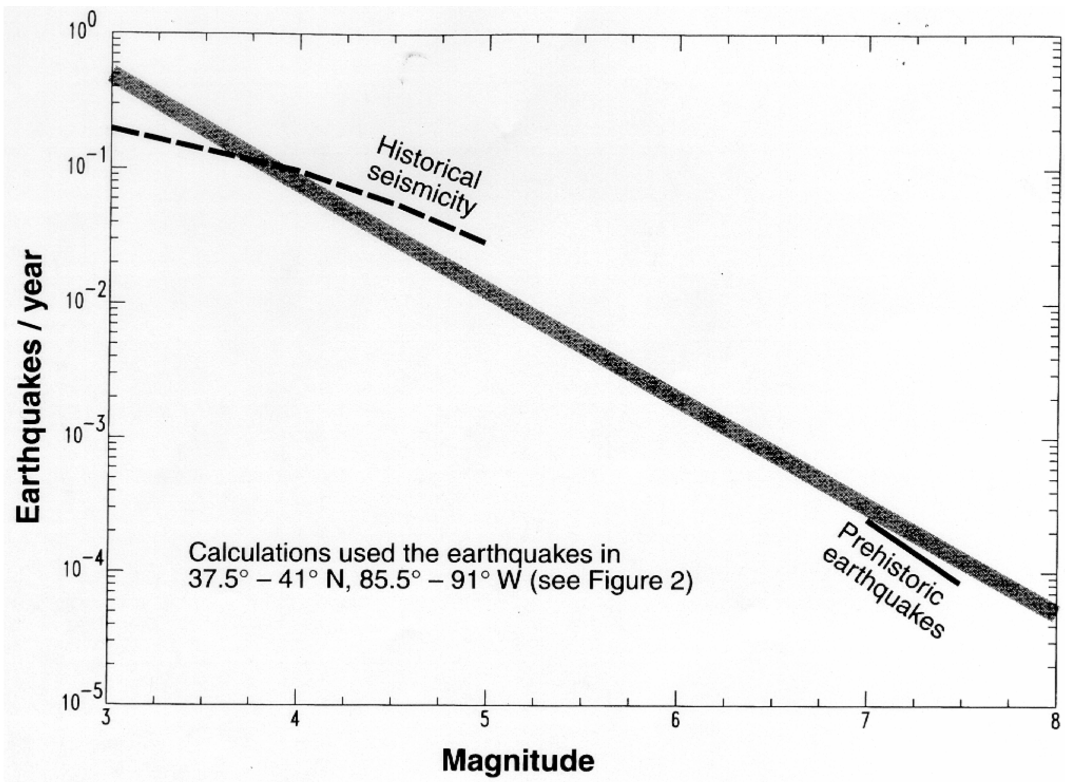

Figure 17. Magnitude-frequency relationship in the Wabash Valley Seismic Zone (Wheeler and Cramer, 2002).

5.0 Ground-Motion Attenuation Relationship

One of the fundamental differences in assessing seismic hazard between the western and central United States is ground motion attenuation relationship (Wang and others, 2005). The attenuation relationships developed in California are all based on real observations, such as Abrahamson and Silva (1997), Boore et al. (1997), Campbell and Bozorgnia (2003), and Sadigh et al. (1997). In contract, all the attenuation relationships currently available in the CUS are all based on theoretical models (EPRI, 2003). This significant difference results in differences in ground motion uncertainties in both median and its standard deviation for the New Madrid seismic zone. As shown by Frankel (2004), the median ground motions for California vary only slightly between proposed attenuation relationships. For example, PGA ranges from 0.30 to 0.38g between four attenuation relationships for an M7.8 earthquake at 15 km in San Francisco (Frankel, 2004). For comparison, Table 4 lists the median ground motions (PGA) for an M7.7 earthquake at 15 km in the New Madrid seismic zone from six attenuation relationships. The range of the median PGA in the CUS is between 0.46 and 1.20g. Similarly, Frankel (2004) also showed the large range of median ground motion, especially in near-source (<30 km). The theoretical models predict higher median ground motions (PGA and 5 Hz S.A.) in the CUS for a similar earthquake. However, the predicted median ground motions themselves are uncertain because there is no observation in the CUS. The theoretical models also predict higher standard deviations in the CUS. The standard deviations are about 0.3-0.5 in California and 0.6-0.8 in CUS.

Table 4. Median ground motions for an M7.7 New Madrid earthquake from several attenuations relationships at 15 km for a hard-rock site.

	Frankel et al. (1996)	Toro et al. (1997)	Atkinson and Boore (1995)	Campbell (2003)	Somerville et al. (2001)
PGA (g)	1.20	0.90	0.90	0.91	0.69

Use of different attenuation relationships will results in different ground motion estimates. As stated by Frankel and others (2002), “significant differences between the 1996 and 2002 maps are caused by the inclusion of additional attenuation relations in the 2002 maps. In 1996, we used the attenuation relations of Toro et al. (1997) and Frankel et al. (1996), which were assigned equal weight. For the 2002 maps we have added the attenuation relations of Atkinson and Boore (1995), Somerville et al. (2001) and Campbell (2003).” There is no consistent or unique way on how to use these ground motion attenuation relationships (SSHAC, 1997). However, there is a clear consensus that many current attenuation relationships may predict high ground motion, particularly in the near-source, particularly Frankel and others’ attenuation relationship (USGS/NRC Workshop, 2005). Figure 18 shows some of the ground-motion attenuation relationships for an M8.0 earthquake in the central United States. In this report, we will use the ground motion attenuation relationships of Somerville and others (2001), Campbell (2003), and Atkinson (2005).

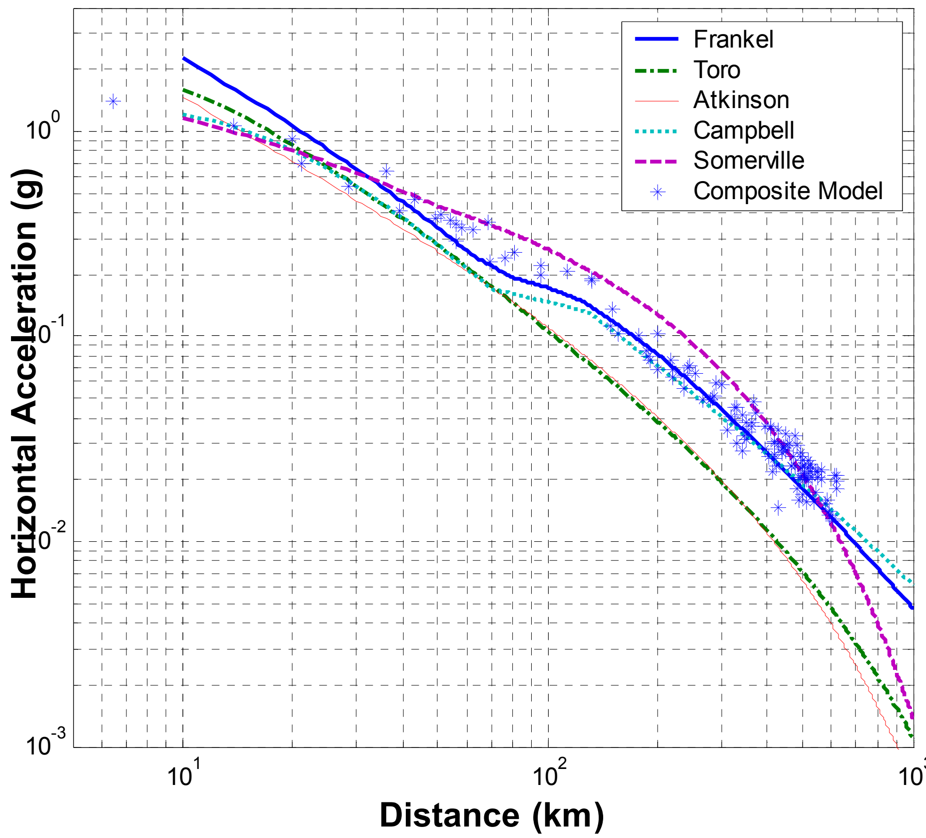

Figure 18. Ground-motion attenuation relationships for an M8.0 earthquake in the central United States.

5.0 Preliminary Results

Figure 19 shows the site (PGDP) and two seismic sources: i.e., the New Madrid fault and Wabash Valley Seismic Zone. The shortest distances from PDGP to the New Madrid fault and Wabash Valley Seismic Zone are 45 and 60 km, respectively. As shown by Frankel and others (2002) and Frankel (2004), seismic hazard at PDGP is dominated by the New Madrid fault. Thus, the following hazard calculations are only for the New Madrid fault with Campbell's (2003) attenuation relationship.

Figure 20 shows the PGA hazard curve derived from current PSHA for the New Madrid characteristic source. PGA with 2 percent PE in 50 years is about 0.5g (Fig. 20). As discussed earlier, there is only one characteristic earthquake of M7.7 with a recurrence interval of 500 years from the New Madrid source. In other words, there should be only one return period (or annual probability of exceedance) for the ground motion, because the ground motion is a consequence of the earthquake. Current PSHA (equation [19]) could derive a range of return periods, from 500 years to infinity, for the characteristic fault, however (Fig. 20). PGA of 10g or even large could be derived by current PSHA. As shown earlier, this is caused by the mathematical error in the formulations of current PSHA.

KY-PSHA (equation [31]) will derive only one return period, 500 years, for the New Madrid characteristic source. The best PGA estimate (median or mean in log) with 500-year return period at PDGP is 0.27g. The median + one standard deviation PGA is 0.54g for this return period. And the median + two standard deviations PGA is 1.09g.

For the single characteristic scenario (earthquake) in the New Madrid zone, DSHA will give the best PGA estimate of 0.27g, median + one standard deviation PGA of 0.54g, and median + two standard deviations PGA of 1.09g.

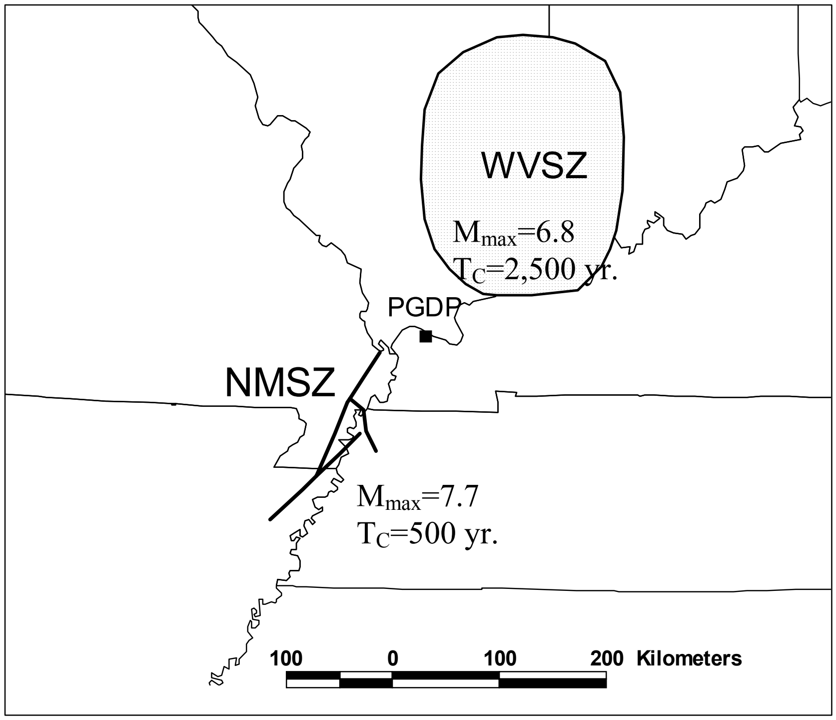

Figure 19. PGDP and seismic sources.

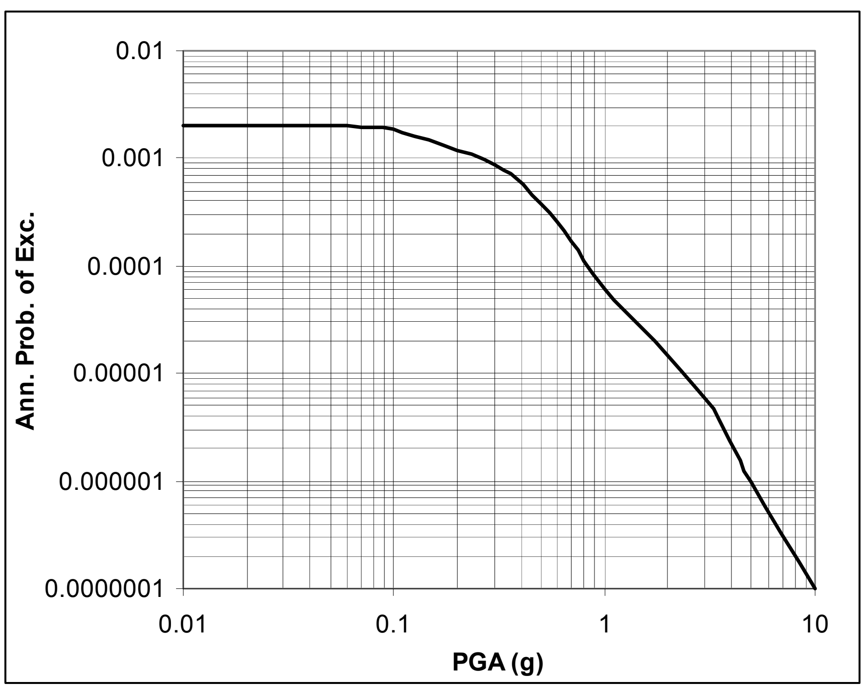

Figure 20. PGA hazard curve at PGDP from the New Madrid fault (45 km).

References

Abrahamson, N.A., and Bommer, J.J. (2005). Probability and uncertainty in seismic hazard analysis, *Earthquake Spectra*, **21**, 603–607.

Abrahamson, N.A. and W.J. Silva, 1997, Empirical response spectral attenuation relations for shallow crustal earthquakes, *Seis. Res. Lett.*, **68**:94-127.

Anderson, C., Z. Wang, and E.W. Woolery, Observed Seismicity in the Jackson Purchase Region of Western Kentucky between January 2003 and June 2005, **the 77th Annual Meeting of the Eastern Section of the Seismological Society of America**, Memphis, Tennessee, October 3-4, 2005.

Atkinson, G.M. (in press), Challenges in seismic hazard analysis for continental interiors, *in* Continental Intraplate Earthquakes, Geological Society of America.

Atkinson, G.M., and D.M. Boore (1997). Some comparisons between recent ground-motion relations *Seism. Res. Lett.*, **64**, 24–40.

Atkinson, G., and D. Boore (1995). New ground-motion relations for eastern North America, Bulletin of the Seismological Society of America 85, 17-30.

Bakun, W.H. and M.G. Hopper (2002). The 1811-12 New Madrid, Missouri, and the 1886 Charleston, South Carolina, earthquakes, in review.

Bear, G.W., J.A. Rupp, and A.J. Rudman (1997). Seismic interpretations of the deepstructure of the Wabash Valley fault system, Seismological Research Letters 68, 624-640.

Bernreuter, D.L., Savy, J.B., Mensing, R.W., and Chen, J.C., 1989, Seismic hazard characterization of 69 nuclear plant sites east of the Rocky Mountains, Report NUREG/CR-5250, vols. 1-8.

Bommer, J.J., N.A. Abrahamson, F.O. Strasser, A. Pecker, P-Y Bard, H. Bungum, F. Cotton, D. Fäh, F. Sabetta, F. Scherbaum, and J. Studer (2004). The challenge of defining upper bounds on earthquake ground motions, *Seism. Res. Lett.*, **75**, 82–95.

Boore, D.M., W.B. Joyner, and T.E. Fumal, 1997, Equations for estimating horizontal response spectra and peak acceleration from western North American earthquakes: A summary of recent work, *Seis. Res. Lett.*, **68**:128-153.

Braile, L.W., Hinze, W.J., Keller, G.R., Lidiak, E.G., and Sexton, J.L., 1986, Tectonic development of the New Madrid rift complex, Mississippi Embayment, North America: Tectonophysics, v. 131, p. 1–21.

Building Seismic Safety Council (BSSC), 2004, NEHRP recommended provisions for seismic regulations for new buildings [2003 ed.]: Federal Emergency Management Agency, FEMA 450, 340 p.

Building Seismic Safety Council (BSSC), 1998, NEHRP recommended provisions for seismic regulations for new buildings [1997 ed.]: Federal Emergency Management Agency, FEMA 302, 337 p.

Building Seismic Safety Council (BSSC) (1995). NEHRP recommended provisions for seismic regulations for new buildings [1994 ed.], Federal Emergency Management Agency, FEMA 222A, 290 p.

Campbell, K.W., 2003, Prediction of strong ground motion using the hybrid empirical

method and its use in the development of ground-motion (attenuation) relations in eastern North America: Bulletin of the Seismological Society of America, v. 93, p. 1,012–1,033.
Campbell, K.W. (1981). Near-source attenuation of peak horizontal acceleration, *Bull. Seismo. Soc. Am.*, **71**, 2,039- 2,070.
Campbell, K.W. and Y. Bozorgnia, 2003, Updated near-source ground motion (attenuation) relations for the horizontal and vertical components of peak ground acceleration and acceleration response spectra, *Bull. Seismo. Soc. Am.*, **93**:314-331.
Chiu, J.-M., A.C. Johnston, and Y.T. Yang (1992). Imaging the active faults of the Central New Madrid Seismic Zone using PANDA array data, Seismological Research Letters 63, 375-393.
Cornell, C.A., 1968, Engineeing seismic risk analysis: Bulletin of the Seismological Society of America, v. 58, p. 1,583–1,606.
Cornell, C.A., 1971, Probabilistic analysis of damage to structures under seismic loads, *in* Howells, D.A., Haigh, I.P., and Taylor, C., eds., Dynamic waves in civil engineering: Proceedings of a conference organized by the Society for Earthquake and Civil Engineering Dynamics: New York, John Wiley, p. 473-493.
Cramer, C.H., 2004b, Earthscope and PSHA 2004, (http://www.ceri.memphis.edu/ usgs/products/ppt_db2.html).
Cramer, C.H., 2004a, Comment on "Communicating with uncertainty: A critical issue with probabilistic seismic hazard analysis" by Z. Wang, Woolery, E.W., Shi, B., and Kiefer, J.D., EOS, Transactions of the American Geophysical Union, v. 85, p 283.
Cramer, C.H., 2001, The New Madrid seismic zone: capturing variability in seismic hazard analyses: *Seis. Res. Lett.*, **72**:664-672.
Electric Power Research Institute (EPRI), 1988, Seismic hazard methodology for central and eastern United States, EPRI NR-4726, vols. 1-10.
Electric Power Research Institute (EPRI), 2003, CEUS ground motion project, model development and results: Report 1008910.
Frankel, A., 2005, Reply to "Comment on 'How Can Seismic Hazard around the New Madrid Seismic Zone Be Similar to that in California?' by Arthur Frankel," by Zhenming Wang, Baoping Shi, and John D. Kiefer: Seismological Research Letters, v.76, p.472–475.
Frankel, A., 2004, How can seismic hazard around the New Madrid Seismic Zone be similar to that in California?: Seismological Research Letters, v. 75, p. 575–586.
Frankel, A., Mueller, C., Barnhard, T., Perkins, D., Leyendecker, E., Dickman, N., Hanson, S., and Hopper, M., 1996, National seismic hazard maps: Documentation June 1996: U.S. Geological Survey Open-File Report 96-532, 110 p.
Frankel, A.D., Petersen, M.D., Mueller, C.S., Haller, K.M., Wheeler, R.L., Leyendecker, E.V., Wesson, R.L., Harmsen, S.C., Cramer, C.H., Perkins, D.M., and Rukstales, K.S., 2002, Documentation for the 2002 Update of the National seismic hazard maps: U.S. Geological Survey Open-File Report 02-420, 33 p.
Geomatrix Consultants, Inc., 2004, Dam safety seismic hazard assessment: Tennessee Valley Authority region, Project 9223, 137p.
Gupta, R.S. (1989) Hydrology and hydraulic systems, Englewood Cliffs, N.J., Prentice-

Hall, 739p.
Herrmann, R.B., and C.J. Ammon (1997). Faulting parameters of earthquakes in the New Madrid, Missouri, region, Engineering Geology 46, 299-311.
Holzer, T.L., 2005, Comment on "Comparison between probabilistic seismic hazard analysis and flood frequency analysis" by Zhenming Wang Lindell Ormsbee: EOS, Transactions of the American Geophysical Union, v. 86, p 303.
Hough, S.E., J.G. Armbruster, L. Seeber, and J.F. Hough (2000). On the Modified Mercalli intensities and magnitudes of the 1811-12 New Madrid earthquakes, *J. Geophys. Res.*, v. 105, pp. 23,839-23,864.
International Code Council (ICC), 2000, International Building Code: 678 p.
Johnston, A.C. (1996a). Seismic moment assessment of stable continental earthquake, III., 1811-182 New Madrid, 1886 Charleston, and 1755 Lisbon, *Geophys. J. Int*., v. 126, pp. 314-344.
Johnston, A.C. (1996b). Seismic moment assessment of earthquakes in stable continental regions—I. Instrumental seismicity, *Geophys. J. Int*., v. 124, pp. 381-414.
Johnston, A.C., and Schweig, E.S., 1996, The enigma of the New Madrid Earthquakes of 1811–1812: Annual Review of Earth and Planetary Sciences, v. 24, p. 339–312.
Kenner, S.J., and Segall, P., 2000, A mechanical model for intraplate earthquakes: Application to the New Madrid Seismic Zone: Science, v. 289, p. 2,329–2,332.
Kim, W. (2003), June 18, 2002 Evansville, Indian Earthquake: Reactivation of ancient rift in the Wabash valley fault zone?, *Bull. Seism. Soc. Am*., v. 93, p2201-2211.
Kramer, S.L. (1996). Geotechnical earthquake engineering, Upper Saddle River, N.J., Prentice Hall, 653p.
Leyendecker, E.V., R.J. Hunt, A.D., Frankel, and K.S. Rukstales, 2000, Development of maximum considered earthquake ground motion maps, *Earthquake Spectra*, v.16, p21-40.
Liu, H. (1991). Wind engineering, a handbook for structural engineers, Englewood Cliffs, N.J., Prentice-Hall, 209p.
McBride, J.H., T.G. Hildenbrand, W.J. Stephenson, and C.J. Potter (2002). Interpreting the earthquake source of the Wabash Valley Seismic Zone (Illinois, Indiana, and Kentucky) from seismic reflection, gravity, and magnetic intensity data, Seismological Research Letters, 73, 660-686.
McGuire, R.K., 1995, Probabilistic seismic hazard analysis and design earthquakes: Closing the loop: Bulletin of the Seismological Society of America, v. 85, p. 1,275-1,284.
McGuire, R.K., 1976, FORTRAN computer program for seismic risk analysis: U.S. Geological Survey Open-File Report 76-67.
Milne, W.G., and Davenport, A.G., 1969, Distribution of earthquake risk in Canada: Bulletin of the Seismological Society of America, v. 59, p. 729–754.
National Research Council (NRC), 1988, Probabilistic seismic hazard analysis, report of the Panel on Seismic Hazard Analysis: Washington, D.C., National Academy Press, 97 p.
Newman, A., Stein, S., Weber, J., Engeln, J., Mao, A., and Dixon, T., 1999, Slow deformation and low seismic hazard at the New Madrid Seismic Zone: Science, v. 284, p. 619–621.

Nuclear Regulatory Commission (NRC) (1997). Regulatory Guide 1.165, Indentification and characterization of seismic sources and determination of safe shutdown earthquake ground motion.

Nuttli, O.W., and R.B. Herrmann (1978). Credible earthquakes in the Central United States, *in* State-of-the Art for Assessing Earthquake Hazards in the United States, U.S. Army Corps of Engineers Geotechnical Lab Report 12, Vicksburg, Miss., 99 pp.

Obermerier, S. F., N. R. Bleuer, C. A. Munson, P. J. Munson, W. S. Martin, K. M. McWilliams, D. A. Tabacznski, J. K. Odum, M. Rubin, and D. L. Eggert (1991), Evidence of strong earthquake shaking in the Lower Wabash Valley from prehistoric liquefaction features, *Science*, *251*, 1061-1063.

Reiter, L. (1990). Earthquake Hazard Analysis, Columbia University Press, NY, 254p.

Risk Engineering, Inc., 1999, Updated probabilistic seismic hazard analysis for the Paducah Gaseous Diffusion Plant, Paducah, Kentucky, Final Report.

Sacks, P., 1978, Wind forces in engineering [2d ed.]: Elmsford, N.Y., Pergamon Press, 400 p.

Sadigh, K., C.Y. Chang, J.A. Egan, F. Makdisi, and R.R. Youngs (1997). Attenuation relationships for shallow crustal earthquakes bases on California strong motion data, *Seism. Res. Lett.,* **68**, 180–189.

Scherbaum, F., J. Bommer, H. Bungum, F. Cotton, and N. Abrahamson (2005). Composite ground-motion models and logic trees: methodology, sensitivities, and uncertainties, *Bull. Seismol. Soc. Am.*, **95**, 1575–1593.

Senior Seismic Hazard Analysis Committee (SSHAC), 1997, Recommendations for probabilistic seismic hazard analysis: Guidance on uncertainty and use of experts: Lawrence Livermore National Laboratory, NUREG/CR-6372, 81 p.

Sexton, J.L., L.W. Braile, W.J. Hinze, and M.J. Campbell (1996). Seismic reflection profiling studies of a buried Precambrian rift beneath the Wabash Valley fault zone, Geophysics 51, 640-660.

Somerville, P., Collins, N., Abrahamson, N., Graves, R., and Saikia, C., 2001, Ground motion attenuation relations for the central and eastern United States: Final report to U.S. Geological Survey.

Stein, R.S., S. Toda, and T. Parsons (2005). A new probabilistic seismic hazard assessment for greater Tokyo [abs.], 2005 American Geophysical Union Fall Meeting, San Francosco, Calif..

Stein, S., and Newman, A., 2004, Characteristic and uncharacteristic earthquakes as possible artifacts: Applications to the New Madrid and Wabash Seismic Zones: Seismological Research Letters, v. 75, p. 173–187.

Stein, S., Tomasello, J., and Newman, A., 2003, Should Memphis build for California's Earthquakes?: EOS, Transactions of the American Geophysical Union, v. 84, p. 177, 184–185.

Stein, S., and Wysession, M., 2003, An introduction to seismology, earthquakes, and earth structure: Maldem, Mass., Blackwell Publishing, 498 p.

Stepp, J.C., I. Wong, J. Whitney, R. Quittmeyer, N. Abrahamson, G. Toro, R. Youngs, K. Coppersmith, J. Savy, T. Sullivan, and Yucca Mountain PSHA project members (2001). Probabilistic seismic hazard analysis for ground motions and

fault displacements at Yucca Mountain, Nevada, *Earthquake Spectra*, **17**, 113–151.
Stover, C.W., and J.L. Coffman (1993). Seismicity of the United States, 1568-1989 (Revised), U.S. Geological Survey Professional Paper 1527, 418 p.
Street, R., and Z. Wang, 2003, Analysis of Strong Motion Records From the University of Kentucky Accelerometers in the New Madrid Seismic Zones: 1990 Through 2001, **Report to the U.S. Geological Survey**, Award Number: 02HQGR0016, 10p.
Structural Engineers Association of Kentucky (SEAOK), 2002, White Paper on Review of the 2002 Kentucky Residential Code (second edition), SEAOK Document WP-01-2.1, 66p.
Toro, G.R., W.J. Silva, R.K. McGuire, and R.B.Herrmann (1992). Probabilsitic seismic hazard mapping of the Mississippi Embayment, Seism. Res. Letts, v. 63, p. 449-475.
Toro, G.R., Abrahamson, N.A., and Schneider, J.F., 1997, Model of strong ground motions from earthquakes in central and eastern North America: Best estimates and uncertainties: Seismological Research Letters, v. 68, p. 41–57.
Tuttle, M.P. and E.S. Schweig (2000). Earthquake potential of the New Madrid seismic zone (abstract), *EOS, Trans. Am. Geophys. U.*, v. 81, S308-309.
Tuttle, M.P., Schweig, E.S., Sims, J.D., Lafferty, R.H., Wolf, L.W., and Haynes, M.L., 2002, The earthquake potential of the New Madrid Seismic Zone: Bulletin of the Seismological Society of America, v. 92, p. 2080–2089.
Wang, Z., in press (b), Understanding seismic hazard and risk assessments: an example in the New Madrid Seismic Zone of the central United States: Proceedings of the 8th National Conference on Earthquake Engineering, April 18–22, 2006, San Francisco, Calif.
Wang, Z., in press (a), Seismic hazard and risk assessment in the intraplate environment: The New Madrid Seismic Zone of the central United States, *in* Continental intraplate earthquakes, Geological Society of America.
Wang, Z., 2005a, Discussion on Problems in the application of the SSHAC probability method or assessing earthquake hazards at Swiss nuclear power plants by Klügel, J.-U., *Engineering Geology* (in press).
Wang, Z., 2005b, Reply to "Comment on 'Comparison between probabilistic seismic hazard analysis and flood frequency analysis' by Zhenming Wang and Lindell Ormsbee" by R. M. W. Musson, *EOS*, *Trans., AGU*, **86** (39), p 354.
Wang, Z., 2005c, Reply to "Comment on 'Comparison between probabilistic seismic hazard analysis and flood frequency analysis' by Zhenming Wang and Lindell Ormsbee" by Thomas L Holzer, *EOS*, *Trans., AGU*, **86** (33), p 303.
Wang, Z., and Ormsbee, L., 2005, Comparison between probabilistic seismic hazard analysis and flood frequency analysis: EOS, Transactions of the American Geophysical Union, v. 86, p. 45, 51–52.
Wang, Z., Woolery, E.W., Shi, B., and Kiefer, J.D., 2005, Comment on "How Can Seismic Hazard around the New Madrid Seismic Zone Be Similar to that in California?" by Arthur Frankel: Seismological Research Letters, v. 76, p. 466–471.
Wang, Z., Woolery, E.W., Shi, B., and Kiefer, J.D., 2004, Reply to "Comment on

‘Communicating with uncertainty: A critical issue with probabilistic seismic hazard analysis’ by Z. Wang, Woolery, E.W., Shi, B., and Kiefer, J.D.” by Cramer, C.H., EOS, Transactions of the American Geophysical Union, v. 85, p 283.

Wang, Z., E.W. Woolery, and B. Shi, 2003b, Observed Seismicity (Earthquake Activity) in the Jackson, Purchase Region of Western Kentucky: January through June 2003, Kentucky Geological Survey, ser. 12, Special Publication 6, 16p.

Wang, Z., Woolery, E.W., Shi, B., and Kiefer, J.D., 2003a, Communicating with uncertainty: A critical issue with probabilistic seismic hazard analysis: EOS, Transactions of the American Geophysical Union, v. 84, p. 501, 506, 508.

Wheeler, R.L. (1997). Boundary separating the seismically active Reelfoot Rift from the sparsely seismic Rough Creek Graben, Kentucky and Illinois, Seismological Research Letters 63, 586-598.

Wheeler, R.L., and C.H. Cramer (2002). Updated seismic hazard in the southern Illinois Basin -- Geological and geophysical foundations for use in the 2002 USGS national seismic-hazard maps, Seismological Research Letters, 73, 776-791.

Wheeler, R.L., and A. Frankel (2000). Geology in the 1996 USGS seismic-hazard maps, central and eastern United States, Seismological Research Letters 71, 273-282.

Wheeler, R.L. and D.M. Perkins (2000). Research, methodology, and applications of probabilistic seismic-hazard mapping of the central and eastern United States—minutes of a workshop on June 13-14, 2000 at St. Louis University, *U.S. Geological Survey, Open-File Report 00-0390*, 18 pp.

Zoback, M.L., 1992, Stress field constraints on intraplate seismicity in eastern North America: Journal of Geophysical Research, v. 97, p. 11,761–11,782.

Zoback, M.D., W.H. Prescott, and S.W. Kroeger (1985). Evidence for lower crustal ductile strain localization in southern New York, Nature 317, 705-707.

Zoback, M.D., M.L. Zoback, V.S. Mount, J. Suppe, J.P. Eaton, J.P. Eaton, J.H. Healy, D. Oppenheimer, P. Reasenberg, L. Jones, C.B. Raleigh, I.G. Wong, O. Scotti, C. Wentworth (1987). New evidence on the state of stress of the San Andreas fault system, Science 238, 1,105-1,111.